

Incremental data compression for PDE-constrained optimization with a data assimilation application

Xuejian Li¹, John R. Singler^{2*}, Xiaoming He²

¹School of Mathematical and Statistical Sciences, Clemson University, Clemson, 29364, SC, USA.

²Department of Mathematics and Statistics, Missouri University of Science and Technology, Rolla, 65409, MO, USA.

*Corresponding author(s). E-mail(s): singlerj@mst.edu;
Contributing authors: xuejial@clemson.edu; hex@mst.edu;

Abstract

We propose and analyze an inexact gradient method based on incremental proper orthogonal decomposition (iPOD) to address the data storage difficulty in time-dependent PDE-constrained optimization, particularly for a data assimilation problem as a detailed demonstration for the key ideas. The proposed method is proved robust by rigorous analysis. We first derive a sharp data compression error estimate of the iPOD with the help of Hilbert-Schmidt operators. Then we demonstrate a numerical PDE analysis to show how to properly choose the Hilbert space for the iPOD data compression so that the gradient error is under control. We further prove that for a convex problem with appropriately bounded gradient error, the inexact gradient method achieves the accuracy level of the optimal solution while not hurting the convergence rate compared with the usual gradient method. Finally, numerical experiments are provided to verify the theoretical results and validate the proposed method.

Keywords: PDE-constrained optimization, incremental proper orthogonal decomposition, data compression, data assimilation

MSC Classification: 49M41 , 35Q93 , 65N21

1 Introduction

Time-dependent PDE-constrained optimization is commonly witnessed in many applications, such as optimal control [1–5], data assimilation [6–9], and other inverse identification problems [10–16]. Gradient-based methods, such as steepest descent, conjugate gradient, and quasi-Newton methods, are the central machinery to solve this type optimization problem, in which calculating the gradient is a key step. To obtain the gradient, one usually needs to solve a forward time-dependent PDE and store all forward solutions for later use in solving a so-called backward adjoint equation. However, during this procedure, the storage of forward solution data is prohibitive when large-scale temporal and spatial simulations are involved [17, 18], which makes the gradient calculation very difficult.

There are multiple candidates to deal with this data storage difficulty, such as checkpoint [19–22], data compression [23–26], and others [27]. The checkpoint method is frequently used to reduce the memory requirement for PDE-constrained optimization; however, this method may largely increase the computation time due to many recalculations [20, 28]. In contrast, data compression, such as proper orthogonal decomposition (POD) [29–32], can save memory effectively for large-scale low-rank data but only introduce minimal extra computational time, which is attractive. The POD is used to handle memory limitations for optimization in the literature [25, 26]. However, it is still new to this field and under-investigated. This paper will thoroughly consider POD as a data compression technique to address the data storage issue for time-dependent PDE-constrained optimization.

The POD attempts to find an optimal low-dimensional basis to best approximate a set of given data, which is usually solved by singular value decomposition (SVD), and the optimal basis (POD modes) consists of the dominant singular vectors. The POD is often referred to as a model order reduction approach to simplify the structure of complicated systems, which has shown numerous applications in simulating ODEs, PDEs, and many other science problems, see e.g., [9, 33–44]. Also, due to the low dimension representation, POD can be considered as a data compression technique to optimize the storage of large-scale data and address computer memory limitations. Unfortunately, many SVD computing methods, such as those in R, Python, and Matlab, are offline and require storing the entire data matrix first before computing the SVD, which still requests large computer memory. To overcome this dilemma, researchers devoted many efforts to figuring out other reasonable SVD computation algorithms [45–51]. The iPOD (or iSVD) is one of the successful algorithms that was first proposed by Brand [29] and afterward significantly extended and improved by others [30–32, 52]. The iPOD uses an online projection to process data column by column and incrementally update the POD until the last column data is processed. Attractively, the used column data is no longer kept and thus there is no necessity to store the data matrix. This computing property is ideal to handle the data storage difficulty for time-dependent PDE-constrained optimization.

Based on a data assimilation problem as the demonstration example, we utilize the iPOD to incrementally produce the POD of the forward PDE solution as it is numerically simulated. Again, one key feature of this step is that once the solution has been used to update the POD it no longer needs to be stored, which allows us to

effectively compress the large-scale solution data. We then decompress the data one by one as it is needed for solving the backward adjoint equation. In this way, the data storage difficulty is addressed and the gradient calculation is possible. This approach is an inexact gradient method since the compressed (approximated) data is involved during calculation, and errors will be introduced to the gradient.

To rigorously regulate the gradient error and demonstrate the robustness of this method, we provide a theoretical analysis. First, we provide an accurate error estimate between the exact and compressed data while iPOD is utilized. The properties of Hilbert-Schmidt operators play a fundamental role in estimation. Second, with suitable Hilbert space for the iPOD, we show that the gradient error introduced by iPOD is under control. To provide insight on properly applying iPOD in different scenarios, the gradient error analysis will be presented based on a linear and a nonlinear PDE constraint, respectively. Third, with an appropriate iPOD setup, we prove that the inexact gradient method reduces memory requirements without hurting the convergence rate and accuracy of the optimal solution compared to the usual gradient method.

The paper is organized as follows. In Section 2, we recall preliminary knowledge. In Section 3, we propose the inexact gradient method based on iPOD data compression for time-dependent PDE-constrained optimization. In Section 4, we prove that the inexact gradient method achieves the optimal solution with similar computational time compared to usual gradient methods. In Section 5, we provide numerical tests to validate the proposed method. Finally, we draw conclusions in Section 6.

2 Preliminaries

This section introduces preliminaries of POD, Hilbert-Schmidt operators, and iPOD (or iSVD).

2.1 POD and Hilbert-Schmidt operators

Denote the norm of a Hilbert space X as $\|\cdot\|_X$ that is induced by inner product $(\cdot, \cdot)_X$. If X is a finite m -dimensional Hilbert space, then X can be viewed as a m -dimensional weighted Euclidean space \mathbb{R}_M^m , i.e., $\forall x, y \in X$, $(x, y)_X = (\vec{x}, \vec{y})_{\mathbb{R}_M^m} = \vec{y}^T M \vec{x}$, where \vec{x} and \vec{y} denote the vector representation of x and y under a given basis of X , \vec{y}^T denotes the transpose of \vec{y} , and M is a positive definite weight matrix. We denote $\mathcal{L}(X, Y)$ as the collection of linear bounded operators that map X to Y . In addition, we denote $\langle \cdot, \cdot \rangle$ as a generic duality pair between a Hilbert space and its dual space.

The POD (or optimal data compression) problem is described as follows: Given a set of functional data $\{u_j\}_{j=1}^n \subset X$ and a value r , $1 \leq r \ll n$, find the r optimal orthonormal basis vectors $\{\Phi_j\}_{j=1}^r \subset X$ such that the data compression error E_r is minimized:

$$E_r = \sum_{j=1}^n \|u_j - \Pi_{X_r} u_j\|_X, \quad (1)$$

where $\Pi_{X_r} : X \mapsto X_r$ is the orthogonal projection onto $X_r = \text{span}\{\Phi_j\}_{j=1}^r \subset X$. In order to solve problem (1), we introduce the POD operator $\mathcal{U} : \mathbb{R}^n \mapsto X$ defined by

$$\mathcal{U}z = \sum_{j=1}^n z_j u_j, \quad z = [z_1 \ z_2 \ \cdots \ z_n]^T \in \mathbb{R}^n. \quad (2)$$

The operator $\mathcal{U} : \mathbb{R}^n \mapsto X$ is finite rank and thus compact and has a SVD: $\mathcal{U}z = \sum_{j=1}^s \sigma_j(z, \eta_j)_{\mathbb{R}^n} \psi_j$, $\forall z \in \mathbb{R}^n$, $s \leq n$. The $\{\sigma_j\}_{j=1}^s$ are the non-zero singular values of \mathcal{U} , the $\{\psi_j\}_{j=1}^s \in X$ and $\{\eta_j\}_{j=1}^s \in \mathbb{R}^n$ are the corresponding singular vectors. It turns out that problem (1) is equivalent to finding the best r rank Hilbert-Schmidt approximation of \mathcal{U} [53, 54]:

$$\min_{K \in \mathcal{L}(\mathbb{R}^n, X), \text{rank}(K)=r} \|\mathcal{U} - K\|_{\text{HS}} = \sum_{j=1}^n \|u_j - \Pi_{X_r} u_j\|_X. \quad (3)$$

The operator K is obtained by the first r^{th} order truncated SVD of \mathcal{U} : $\mathcal{U}_r z = \sum_{j=1}^r \sigma_j(z, \eta_j)_{\mathbb{R}^n} \psi_j$, $\forall z \in \mathbb{R}^n$, $r \leq s$, and the singular vectors $\{\psi_j\}_{j=1}^r$ are the r optimal basis vectors $\{\Phi_j\}_{j=1}^r$ to solve problem (1). The optimal truncation error (or data compression error) E_r is equal to:

$$E_r = \sum_{j=1}^n \|u_j - \Pi_{X_r} u_j\|_X^2 = \|\mathcal{U} - \mathcal{U}_r\|_{\text{HS}}^2 = \sum_{j=r+1}^n \sigma_j^2. \quad (4)$$

For more understanding of SVD, POD, and Hilbert-Schmidt operators, one can refer to [55, 56].

As illustrated in (3)-(4), Hilbert-Schmidt operators are important machinery for solving the POD problem. We here briefly introduce Hilbert-Schmidt operators and their properties, which will be useful for the analysis later.

Definition 1. Let X and Y be separable Hilbert spaces. An operator $B \in \mathcal{L}(X, Y)$ is Hilbert-Schmidt if

$$\sum_{j \geq 1} \|Bx_j\|_Y^2 < \infty \quad \text{for any total orthonormal sequence } \{x_j\}_{j \geq 1} \subset X. \quad (5)$$

The Hilbert-Schmidt norm of B is defined by $\|B\|_{\text{HS}} = (\sum_{j \geq 1} \|Bx_j\|_Y^2)^{\frac{1}{2}}$.

Lemma 1. [57, Section V] Let X and Y be separable Hilbert spaces. If an operator $B \in \mathcal{L}(X, Y)$ is compact and its singular values $\{\sigma_j\}_{j \geq 1}$ satisfy $\sum_{j \geq 1} \sigma_j^2 < \infty$, then B is Hilbert-Schmidt and $\|B\|_{\text{HS}}^2 = \sum_{j \geq 1} \sigma_j^2$.

Remark 1. Hilbert-Schmidt operators are compact, but not all compact operator are Hilbert-Schmidt.

Since \mathcal{U} defined by (2) is finite rank and thus Hilbert-Schmidt and compact, one can further verify the following Lemma with help of Definition 1.

Lemma 2. [58, Lemma A.3] \mathcal{U} is Hilbert-Schmidt and $\|\mathcal{U}\|_{\text{HS}}^2 = \sum_{j=1}^n \|u_j\|_X^2$.

Since $\text{Range}(U)$ belongs to a finite dimension Hilbert space $X = \mathbb{R}_M^m$ with prescribed basis, the operator U can be represented by the matrix $U : \mathbb{R}^n \mapsto \mathbb{R}_M^m$ given by $U = [\vec{u}_1 \ \vec{u}_2 \ \cdots \ \vec{u}_n]$. In this sense, we denote $\|U\|_{\text{HS}} = \|\mathcal{U}\|_{\text{HS}}$. The Hilbert adjoint operator of $U : \mathbb{R}^n \mapsto \mathbb{R}_M^m$ is $U^* : \mathbb{R}_M^m \mapsto \mathbb{R}^n$ given by $U^* = U^T M$, which is verified via $(U\vec{x}, \vec{y})_{\mathbb{R}_M^m} = \vec{y}^T M U \vec{x} = (U^T M \vec{y})^T \vec{x} = (\vec{x}, U^* \vec{y})_{\mathbb{R}^n}$, $\forall \vec{x} \in \mathbb{R}_M^m, \vec{y} \in \mathbb{R}^n$. Thus, for different Hilbert space X or weight matrix M , the SVD of U will be different. In general, we define the SVD of $U : \mathbb{R}^n \mapsto \mathbb{R}_M^m$ as follows:

Definition 2. *The core M -weighted SVD of a matrix $U_{m \times n} : \mathbb{R}^n \mapsto \mathbb{R}_M^m$ is a decomposition $U = V \Sigma W^T$, where $V \in \mathbb{R}^{m \times s}$, $\Sigma \in \mathbb{R}^{s \times s}$, and $W \in \mathbb{R}^{n \times s}$ satisfy*

$$V^T M V = I, \quad \Sigma = \text{diag}(\sigma_1, \sigma_2, \dots, \sigma_s), \quad W^T W = I. \quad (6)$$

Here, $\sigma_1 \geq \sigma_2 \geq \dots \geq \sigma_s > 0$ are positive singular values of U , and the column of V and W are the left and right singular vectors of U .

In Definition 2, we follow [30, Definition 2.1] and use the terminology ‘‘core’’ to exclude the zero singular values since POD does not need information from zero singular values for data compression. We refer to the SVD of $U : \mathbb{R}^n \mapsto \mathbb{R}^m$ ($M = I$) as the core standard SVD and the SVD of $U : \mathbb{R}^n \mapsto \mathbb{R}_M^m$ ($M \neq I$) as the core M -weighted SVD, in order to distinguish the SVD of U with standard and weighted Euclidean range spaces. Also, we refer to the matrix W in (6) satisfying $W^T W = I$ as a standard orthonormal matrix and the matrix V satisfying $V^T M V = I$ as an M -orthonormal matrix, respectively.

Based on SVD and equations (1)-(4), what POD attempts to obtain is:

$$U_{m \times n} \approx V_{m \times r} \Sigma_{r \times r} (W_{n \times r})^T \quad r < s \text{ with } r \ll n, \text{ and} \quad (7)$$

$$V^T M V = I, \quad \Sigma_r = \text{diag}(\sigma_1, \sigma_2, \dots, \sigma_r), \quad W^T W = I. \quad (8)$$

Compared to (6), which removes the zero singular values, the nonzero singular values $\sigma_{r+1}, \dots, \sigma_s$ and the corresponding singular vectors may also be truncated because of their small magnitudes. Consequently, all matrices $V_{m \times r}$, $\Sigma_{r \times r}$, and $W_{r \times n}$ are easier to be stored due to their smaller size. This is why POD can be used to optimize data storage and reduce memory requirements.

2.2 Incremental proper orthogonal decomposition

The iPOD uses an online projection and QR decomposition to process data one by one and compute the POD (or SVD). The main strength of iPOD is that it does not require pre-storing the entire data matrix, which was proposed by Brand for data in standard Euclidean space \mathbb{R}^m [29] and then extended to data in a general finite-dimensional Hilbert space \mathbb{R}_M^m to deal with functional data [30–32]. We here recall the iPOD for data in general finite-dimensional Hilbert space, which primarily summarizes development in literature [29–32]. Especially, we consider a block-wise data processing [52] to reduce the loss of orthogonality issue [29–32] that often happens to the POD basis due to accumulated round-off error from many matrix multiplications.

To start, we provide a few matrix notations: For a matrix M , let $M_{(:,c:d)}$ denote the submatrix with the columns $c, c+1, \dots, d$ of M , let $M_{(c:d,:)}$ denote the submatrix with the rows $c, c+1, \dots, d$ of M , let $M_{(a:b,c:d)}$ denote a submatrix that has elements belonging to both rows $a, a+1, \dots, b$ and columns $c, c+1, \dots, d$ of M .

Let U be a data matrix and $U = V_{m \times l} \Sigma_{l \times l} W_{j \times l}^T$ be the core M -weighted SVD and \vec{u}^{j+1} be a new column data available to be processed. We first project \vec{u}^{j+1} onto V :

$$\underbrace{VV^* \vec{u}^{j+1}}_{\text{projecting } \vec{u}^{j+1} \text{ onto } V} \implies \underbrace{\tilde{e} = \vec{u}^{j+1} - VV^* \vec{u}^{j+1}}_{\text{new orthogonal vector}} \implies e = \underbrace{\frac{\tilde{e}}{\|\vec{u}^{j+1} - VV^* \vec{u}^{j+1}\|_{\mathbb{R}_M^m}}}_{\text{normalization}}. \quad (9)$$

Let $p = \|\vec{u}^{j+1} - VV^* \vec{u}^{j+1}\|_{\mathbb{R}_M^m}$. We then decompose the new matrix $[U \ \vec{u}^{j+1}]$ as:

$$\begin{aligned} [U \ \vec{u}^{j+1}] &= [V \Sigma W^T \ \vec{u}^{j+1}] = [V \ e] \underbrace{\begin{bmatrix} \Sigma W^T & V^* \vec{u}^{j+1} \\ 0 & p \end{bmatrix}}_{\text{QR decomposition}} \\ &= [V \ e] \begin{bmatrix} \Sigma & V^* \vec{u}^{j+1} \\ 0 & p \end{bmatrix} \begin{bmatrix} W^T & 0 \\ 0 & 1 \end{bmatrix}. \end{aligned} \quad (10)$$

Let tol_p be a user-defined threshold that defines an acceptable amount of approximate linear dependence between \vec{u}^{j+1} and V .

p-truncation: If $p = \|\vec{u}^{j+1} - VV^* \vec{u}^{j+1}\|_{\mathbb{R}_M^m} < \text{tol}_p$, we approximately consider that the new data \vec{u}^{j+1} is linearly dependent on V , i.e., $p \approx 0$ or $\vec{u}^{j+1} \approx VV^* \vec{u}^{j+1}$. Assume the consecutive available data $\vec{u}^{j+1}, \vec{u}^{j+2}, \dots, \vec{u}^{j+d}$ are all approximately linearly dependent on V . Based on the decomposition in (10), all e and p generated by $\vec{u}^{j+1}, \vec{u}^{j+2}, \dots, \vec{u}^{j+d}$ are zero. We then have [52]:

$$[U \ \vec{u}^{j+1} \ \dots \ \vec{u}^{j+d}] \approx V [\Sigma \ V^* \vec{u}^{j+1} \ \dots \ V^* \vec{u}^{j+d}] \begin{bmatrix} W^T & 0 \\ 0 & I_d \end{bmatrix}. \quad (11)$$

Let $Q = [\Sigma \ V^* \vec{u}^{j+1} \ V^* \vec{u}^{j+2} \ \dots \ V^* \vec{u}^{j+d}]$ and $Q = V_Q \Sigma_Q W_Q^T$ be the core standard SVD. We then have

$$\begin{aligned} [U \ \vec{u}^{j+1} \ \dots \ \vec{u}^{j+d}] &\approx V V_Q \Sigma_Q W_Q^T \begin{bmatrix} W^T & 0 \\ 0 & I_d \end{bmatrix} \\ &= (V V_Q) \Sigma_Q \left(\begin{bmatrix} W & 0 \\ 0 & I_d \end{bmatrix} W_Q \right)^T. \end{aligned} \quad (12)$$

It is not difficult to verify that $V V_Q$ is M -orthonormal, Σ_Q is ordered diagonal, and $\begin{bmatrix} W & 0 \\ 0 & I_d \end{bmatrix} W_Q$ is standard orthonormal, which tells us that $[U \ \vec{u}^{j+1} \ \dots \ \vec{u}^{j+d}] \approx (V V_Q) \Sigma_Q \left(\begin{bmatrix} W & 0 \\ 0 & I_d \end{bmatrix} W_Q \right)^T$ is the approximated core M -weighted SVD. Also, note

that $\begin{bmatrix} W & 0 \\ 0 & I_d \end{bmatrix} W_Q = \begin{bmatrix} W & 0 \\ 0 & I_d \end{bmatrix} \begin{bmatrix} W_{Q(1:l,1:l)} \\ W_{Q(l+1:l+d,1:l)} \end{bmatrix} = \begin{bmatrix} WW_{Q(1:l,:)} \\ W_{Q(l+1:l+d,:)} \end{bmatrix}$. Therefore, we update the POD as:

$$V \leftarrow VV_Q, \quad \Sigma \leftarrow \Sigma_Q, \quad W \leftarrow \begin{bmatrix} WW_{Q(1:l,:)} \\ W_{Q(l+1:l+d,:)} \end{bmatrix}. \quad (13)$$

SV-truncation: If $p = \|\bar{u}^{j+1} - VV^*\bar{u}^{j+1}\|_{\mathbb{R}_M^m} \geq \text{tol}_p$, the new data \bar{u}^{j+1} is linearly independent on V . Continuing on (10), we let $\tilde{Q} = \begin{bmatrix} \Sigma & V^*\bar{u}^{j+1} \\ 0 & p \end{bmatrix}$ and $\tilde{Q} = \tilde{V}_Q \tilde{\Sigma}_Q \tilde{W}_Q^T$ be the core standard SVD. Then the matrix $[U \ \bar{u}^{j+1}]$ is decomposed as:

$$\begin{aligned} [U \ \bar{u}^{j+1}] &= [V \ e] \tilde{V}_Q \tilde{\Sigma}_Q \tilde{W}_Q^T \begin{bmatrix} W^T & 0 \\ 0 & 1 \end{bmatrix} \\ &= ([V \ e] \tilde{V}_Q) \tilde{\Sigma}_Q \left(\begin{bmatrix} W & 0 \\ 0 & 1 \end{bmatrix} \tilde{W}_Q \right)^T. \end{aligned} \quad (14)$$

Again, one can easily check that $[V \ e] \tilde{V}_Q$ is M -orthonormal, $\tilde{\Sigma}_Q$ is ordered diagonal, and $\begin{bmatrix} W & 0 \\ 0 & 1 \end{bmatrix} \tilde{W}_Q$ is standard orthonormal.

Let $\Sigma = \text{diag}(\lambda_1, \lambda_2, \dots, \lambda_l)$ and $\tilde{\Sigma}_Q = \text{diag}(\mu_1, \mu_2, \dots, \mu_{l+1})$. According to [52, Lemma 3], we have the following relationship among $\{\lambda_i\}$, $\{\mu_i\}$ and p :

$$\mu_{l+1} \leq p, \quad \mu_{l+1} \leq \lambda_l \leq \mu_l \leq \lambda_{l-1} \cdots \mu_2 \leq \lambda_1. \quad (15)$$

The inequalities in (15) inform us that the singular value μ_{l+1} may be small and negligible. Thus, we may truncate μ_{l+1} and the corresponding singular vectors. Let tol_{sv} be a user-defined threshold of the singular value truncation (SV-truncation). If $\mu_{l+1} < \text{tol}_{sv}$, we apply SV-truncation and have the POD update:

$$V \leftarrow [V \ e] \tilde{V}_{Q(:,1:l)}, \quad \Sigma \leftarrow \tilde{\Sigma}_{Q(1:l,1:l)}, \quad W \leftarrow \begin{bmatrix} W & 0 \\ 0 & 1 \end{bmatrix} \tilde{W}_{Q(:,1:l)}. \quad (16)$$

Exact update: If $p = \|\bar{u}^{j+1} - VV^*\bar{u}^{j+1}\|_{\mathbb{R}_M^m} \geq \text{tol}_p$ and $\mu_{l+1} \geq \text{tol}_{sv}$, then no truncation is applied. We thus have the exact POD update:

$$V \leftarrow [V \ e] \tilde{V}_Q, \quad \Sigma \leftarrow \tilde{\Sigma}_Q, \quad W \leftarrow \begin{bmatrix} W & 0 \\ 0 & 1 \end{bmatrix} \tilde{W}_Q. \quad (17)$$

The formulas (13), (16), and (17) are the foundation for the iPOD Algorithm. We summarize (9)-(17) in Algorithm 1.

Remark 2. In Algorithm 1, the projection to generate “ e ” may contain round-off error so that the matrix $[V \ e]$ is not M -orthonormal. We simply check and fix this issue by projecting multiple times [59]; see lines 16 – 19 in Algorithm 1.

Algorithm 1 iPOD Algorithm

```
1: Initialization:  $d = 0$ ,  $e_p = 0$ ,  $e_{sv} = 0$ ,  $V_0 = 1$ ,  $V = \frac{\vec{u}^1}{\|\vec{u}^1\|_{\mathbb{R}_M^m}}$ ,  $\Sigma = \|\vec{u}^1\|_{\mathbb{R}_M^m}$ , and  
    $W = 1$ ;  
2: Input:  $\vec{u}^{j+1}$ ,  $M$ ,  $V_{m \times l}$ ,  $\Sigma_{l \times l}$ ,  $W_{j \times l}$ ,  $V_0$ ,  $\text{tol}_p$ ,  $\text{tol}_{sv}$ ,  $\text{tol}_o$ ,  $d$ ,  $e_p$ ,  $e_{sv}$ ;  
3: Compute  $\vec{b} = V^T M \vec{u}^{j+1}$ ,  $\tilde{e} = \vec{u}_{j+1} - V \vec{b}$ ,  $p = \|\tilde{e}\|_{\mathbb{R}_M^m}$ ;  
4: if  $p < \text{tol}_p$  &  $j < n$  then  
5:    $d = d + 1$ ;  
6:    $B_{(:,d)} = \vec{b}$ ;  
7:    $e_p = e_p + p$ ; % Data compression error from  $p$ -truncation  
8: else  
9:   if  $d > 0$  then  
10:    Compute the core standard SVD of  $Q$ :  $[\Sigma \ B] = V_Q \Sigma_Q W_Q$ ;  
11:     $V_0 = V_Q$ ;  
12:    Update:  $\Sigma = \Sigma_Q$ ,  $W = \begin{bmatrix} W W_{Q(1:l,:)} \\ W_{Q(l+1:l+d,:)} \end{bmatrix}$ ;  
13:    Update:  $\vec{b} = V_Q^T \vec{b}$ ;  
14:   end if  
15:   Set  $e = \frac{\tilde{e}}{p}$ ;  
16:   while  $V(:, 1)^T M e > \text{tol}_o$  do  
17:      $e = e - V V^T M e$ ;  
18:      $e = \frac{e}{\|e\|_{\mathbb{R}_M^m}}$ ;  
19:   end while  
20:   Set  $V = [V \ e]$ ,  $\tilde{Q} = \begin{bmatrix} \Sigma & \vec{b} \\ 0 & p \end{bmatrix}$ ;  
21:   Compute the core standard SVD of  $\tilde{Q}$ :  $= \tilde{V}_Q \tilde{\Sigma}_Q \tilde{W}_Q$ ;  
22:   Set  $V_1 = \begin{bmatrix} V_0 & 0 \\ 0 & 1 \end{bmatrix}$ ;  
23:   if  $\tilde{\Sigma}_{Q(l+1,l+1)} > \text{tol}_{sv}$  then  
24:     Update:  $V = [V \ e] V_1 \tilde{V}_Q$ ,  $\Sigma = \tilde{\Sigma}_Q$ ,  $W = \begin{bmatrix} W & 0 \\ 0 & 1 \end{bmatrix} \tilde{W}_Q$ ,  $V_0 = I_{l+1}$ ;  
25:   else  
26:     Update:  $\tilde{V}_Q = V_1 \tilde{V}_Q$ ,  $V = [V \ e] \tilde{V}_{Q(:,1:l)}$ ,  $\Sigma = \tilde{\Sigma}_{Q(1:l,1:l)}$ ,  
        $W = \begin{bmatrix} W & 0 \\ 0 & 1 \end{bmatrix} \tilde{W}_{Q(:,1:l)}$ ,  $V_0 = I_l$ ;  
27:      $e_{sv} = e_{sv} + \tilde{\Sigma}_{Q(l+1,l+1)}$ ; % Data compression error from SV-truncation  
28:   end if  
29:    $B = [ \ ]$ ,  $d = 0$ ;  
30: end if  
31: Return:  $V = V$ ,  $\Sigma = \Sigma$ ,  $W = W$ ,  $d$ ,  $e_p$ ,  $e_{sv}$ ,  $V_0$ ;
```

In line 7 and line 27, we propose an incremental way to calculate the data compression error from p -truncation and SV -truncation. We prove in Section 4.1 that this is a sharp estimate for the data compression error.

Also, note that this block-wise data treatment in (11) does not cause any storage issue even for large d since the matrix $[\Sigma V^* \vec{u}^{j+1} V^* \vec{u}^{j+2} \dots V^* \vec{u}^{j+d}]$ is normally a wide-short small size matrix.

Algorithm 1 differs from classical iPOD algorithms [29–32] primarily in lines 4–14. The classical iPOD Algorithms update the POD basis V by matrix multiplication as every new column data comes in and will encounter loss of orthogonality on V quickly due to accumulated round-off error. Hence, the Gram-Schmidt procedure must be applied often to reorthogonalize V , which is the most computationally expensive step in classical iPOD. On the other hand, the block-wise processing of p -truncation data from [52] in Algorithm 1 only involves one-time matrix multiplication to update the V and W for d columns data, which largely reduces the source of round-off error, preserves the orthogonality of V , and allows us to obtain accurate POD with less cost.

3 iPOD data compression for time-dependent PDE-constrained optimization

Next, we present the iPOD data compression for the optimization problem with time-dependent PDE constraint, by using a data assimilation problem for the detailed demonstration. From now on, let V and H denote separable Hilbert spaces. Let $V \subset H \subset V'$ be a triplet over a domain Ω , where V' is the dual space of V . The function spaces $L^2(0, T; X)$ and $L^\infty(0, T; X)$ are given by $L^2(0, T; X) := \{v \mid v(t) \in X \text{ for a.e. } t \in (0, T) \text{ and } \int_0^T \|v\|_X^2 dt < \infty\}$ and $L^\infty(0, T; X) := \{v \mid v(t) \in X \text{ and } \|v(t)\|_X < \infty \text{ for a.e. } t \in (0, T)\}$. A time-dependent PDE is generally written as (after suppressing the boundary conditions):

$$\begin{cases} \frac{\partial u}{\partial t} + Au + F(u) = f & \text{in } V' \\ u(\cdot, 0) = u_0 & \text{in } H. \end{cases} \quad (18)$$

Here, $A : V \mapsto V'$ and $F : V \mapsto V'$ are generic linear and nonlinear operators.

Time-dependent PDE-constrained optimization problems have many applications, and each application may involve different formulations with respect to either the objective function or the constraint. Nevertheless, the use of iPOD will all happen in the same step that compresses the forward solution data to save storage and make the gradient calculation possible. In this paper, we concretely consider a data assimilation problem, which is a data-driven solution discovery problem involving initial identification, as a typical example of the PDE-constrained optimization for presentation. The iPOD data compression and the analysis can certainly be extended to other types of optimization problems with time-dependent PDE constraints, which is interesting future work.

In this paper, we focus on the iPOD data compression for the following data assimilation problem. Assume the initial condition u_0 in equation (18) is unknown.

We utilize observation data $\hat{u} \in L^2(0, T; \mathcal{H})$ and the PDE to attempt to identify u_0 and the corresponding solution u by considering the optimization problem [4, 60, 61]

$$\min_{u_0 \in \mathcal{U}} J(u_0) = \frac{1}{2} \int_0^T \|\hat{u} - \mathcal{C}u\|_{\mathcal{H}}^2 dt + \frac{\gamma}{2} \|u_0\|_{\mathcal{U}}^2 \quad \text{subject to (18)}. \quad (19)$$

Here, $\mathcal{C} : V \mapsto \mathcal{H}$ is an observation operator, and \mathcal{H} and \mathcal{U} are Hilbert spaces.

At the discrete level, the problem (19) can be approximated as:

$$\min_{u_{0,h} \in \mathcal{U}_h} J(u_{0,h}) = \frac{1}{2} \tau \sum_{j=1}^n \|\hat{u}^n - \mathcal{C}^j u_h^j\|_{\mathcal{H}}^2 + \frac{\gamma}{2} \|u_{0,h}\|_{\mathcal{U}}^2. \quad (20)$$

subject to

$$\begin{cases} \frac{u_h^{j+1} - u_h^j}{\tau} + Au_h^{j+1} + F(u_h^{j+1}) = f^{j+1} & \text{in } V_h', \\ u_h^0 = u_{0,h} & \text{in } H, \end{cases} \quad (21)$$

for all $j = 0, 1, \dots, n-1$. Here, $\mathcal{C}^j : V \mapsto \mathcal{H}$ is an observation operator, and \mathcal{U}_h is a discrete subspace of \mathcal{U} . Note that in (21) backward Euler is used for the temporal discretization of the PDE constraint (18). The operators A and F involve the spatial discretization, and we still denoted them by A and F . The index $j = 0, 1, 2, 3, \dots, n-1$ represents the time moment, τ is the time step size, and h is the spatial mesh size of the utilized numerical methods, such as the finite element (FE) methods, finite difference methods, or finite volume methods. In the rest of the paper, we consider FE discretization and the FE space is accordingly denoted by $V_h = \text{span}\{\phi_1, \phi_2, \dots, \phi_m\}$, where $\{\phi_i\}$ is a generic FE basis. For $\forall v_h \in V_h$, we have $v_h = \sum_{i=1}^m a_i \phi_i$ and $\vec{v}_h = [a_1 \ a_2 \ \dots \ a_m]^T$ is the vector representation of v_h .

Again, gradient methods, such as steepest descent, conjugate gradient, and quasi-Newton methods, are common mechanisms to solve the problem (20)-(21), which all require calculating the gradient of (20) at $u_{0,h}$ by $j = 0, 1, 2, \dots, n-1$ [62]

$$\begin{cases} \frac{u_h^{j+1} - u_h^j}{\tau} + Au_h^{j+1} + F(u_h^{j+1}) = f^{j+1}, \\ u_h^0 = u_{0,h}, \end{cases} \quad (22)$$

$$\begin{cases} -\frac{u_h^{*j+1} - u_h^{*j}}{\tau} + A^* u_h^{*j} + \left(F'(u_h^{j+1})\right)^* u_h^{*j} = \mathcal{C}^{j+1*} \Lambda(\hat{u}^{j+1} - \mathcal{C}^{j+1} u_h^{j+1}), \\ u_h^{*n} = 0, \end{cases} \quad (23)$$

$$\nabla J(u_{0,h}) = -u_h^{*0}|_{\mathcal{U}_h} + \gamma u_{0,h}, \quad (24)$$

where A^* and \mathcal{C}^{j+1*} are the adjoint operator of A and \mathcal{C}^{j+1} , Λ is the canonical isomorphism of \mathcal{H} and its dual space, $\left(F'(u_h^{j+1})\right)^* u_h^{*j}$ denotes the adjoint of the derivative of F at u_h^{j+1} acting on u_h^{*j} , and $u_h^{*0}|_{\mathcal{U}_h}$ satisfies $(u_h^{*0}, v)_H = (u_h^{*0}|_{\mathcal{U}}, v_h)_{\mathcal{U}} \quad \forall v_h \in \mathcal{U}_h$.

In the rest of the paper, we use the steepest descent method as a representative of gradient-based methods to illustrate using the iPOD data compression approach. The steepest descent method states that:

$$u_{0,h}^{(i+1)} = u_{0,h}^{(i)} - \kappa \nabla J(u_{0,h}^{(i)}), \quad (25)$$

where i is the i^{th} gradient iteration and κ is a positive constant called the descent step size or learning rate.

We summarize the steepest descent method in Algorithm 2.

Algorithm 2 Steepest Descent Algorithm

Input: $u_{0,h}^{(0)}$, and tol_{sd} ; % tol_{sd} denotes the termination tolerance
Set error = 1 and $i = 0$.
while error > tol_{sd} **do**
 Forward phase: solve equation (22) forward with initial $u_{0,h}^{(i)}$ to obtain $\{u_h^{j(i)}\}_{j=1}^n$;
 Backward phase: solve equation (23) backward with $\{u_h^{j(i)}\}_{j=1}^n$ to obtain $u_h^{*0(i)}$;
 Update: $u_{0,h}^{(i+1)} = u_{0,h}^{(i)} - \kappa \nabla J(u_{0,h}^{(i)})$;
 Set $i = i + 1$ and error = $\kappa \|\nabla J(u_{0,h}^{(i)})\|_H$;
end while
Return: $\{u^{j(i)}\}_{j=0}^n$;

In Algorithm 2, the storage of the solution data $\{u_h^{j(i)}\}_{j=1}^n$ (or data matrix $\begin{bmatrix} \bar{u}_h^{1(i)} & \bar{u}_h^{2(i)} & \dots & \bar{u}_h^{n(i)} \end{bmatrix}$ under a prescribed FE basis) at each iteration is problematic when the forward PDE simulation is large-scale. Hence, we apply iPOD at the forward phase to compress the data $\begin{bmatrix} \bar{u}_h^{1(i)} & \bar{u}_h^{2(i)} & \dots & \bar{u}_h^{n(i)} \end{bmatrix}$ to a smaller size, and then decompress it step by step as needed for solving equation (23) to obtain $u_h^{*0(i)}$ and the gradient $\nabla J(u_{0,h}^{(i)}) = u_h^{*0(i)}|_{\mathcal{U}_h} - \gamma u_{0,h}^{(i)}$. This is an inexact gradient method because there is a gradient error at each iteration from solving the backward equation with approximated data of $\{u^{j(i)}\}_{j=1}^n$.

We present this inexact gradient method in Algorithm 3.

Remark 3. *Note that, in the Forward phase of Algorithm 3, we have not provided the weight matrix M yet for iPOD; this will be discussed and provided rigorously through analysis in the following sections.*

In addition, in the Backward phase, to reconstruct $u_h^{j(i)}$ from V, Σ , and W , we first get the vector by $\bar{u}_h^{j(i)} = \frac{1}{\tau} (V\Sigma) W_{(j,:)}^T$ and then obtain $u_h^{j(i)}$ by expanding vector $\bar{u}_h^{j(i)}$ with the given FE basis $\{\phi_i\}_{i=1}^m$.

This inexact gradient method is memory-friendly since we only need to store small size matrices V, Σ , and W instead of $\{\bar{u}_h^{j(i)}\}_{j=1}^n$. However, the gradient $\nabla J(u_{0,h}^{(i)})$ at each iteration has error due to the data compression. Hence, before applying Algorithm 3, we need to answer a few critical questions: Does the inexact gradient method still

Algorithm 3 Inexact Gradient Algorithm

Input: $u_{0,h}^{(0)}$, and tol_{sd} ;

Set $\text{error} = 1$ and $i = 0$.

while $\text{error} > \text{tol}_{sd}$ **do**

Forward phase: implement iPOD Algorithm 1 step by step as data $\{\bar{u}_h^{j(i)}\}$, $j = 1, 2, \dots, n$, becomes available from forward solving (22) with initial $u_{0,h}^{(i)}$ and obtain the compressed data matrix $V\Sigma W^T \approx [\bar{u}_h^{1(i)} \ \bar{u}_h^{2(i)} \ \dots \ \bar{u}_h^{n(i)}]$;

Backward phase: use V, Σ , and W to reconstruct $\{u_h^{j(i)}\}$, $j = n, n-1, \dots, 1$ step by step to solve the backward equation (23) and obtain $u_h^{*0(i)}$;

Update: $u_{0,h}^{(i+1)} = u_{0,h}^{(i)} - \kappa \nabla J(u_{0,h}^{(i)})$;

Set $i = i + 1$ and $\text{error} = \kappa \|\nabla J(u_{0,h}^{(i)})\|_H$;

end while

Return: $\{u^{j(i)}\}_{j=0}^n$;

converge to the optimal solution? If so, how does the convergence behave? We will resolve these concerns with a complete analysis in next section.

4 Analysis for the inexact gradient method

The analysis consists of three steps: iPOD data compression error estimate \rightarrow gradient error analysis \rightarrow convergence of the inexact gradient method. Hilbert-Schmidt operators will be vital in estimating the iPOD data compression error. Using a numerical PDE analysis, we analyze and bound the gradient error by the data compression error. Finally, the gradient error bound and a convex optimization analysis allow us to prove convergence of the inexact gradient method. This analysis framework is generally applicable for any PDE-constrained optimization. The details may differ based on the different PDE problems or gradient methods considered.

4.1 iPOD data compression error estimate

The authors of [31] provide an iPOD error estimate between the exact and compressed data with respect to the infinity matrix norm. We obtain a natural improvement using on the Hilbert-Schmidt norm, since the relevant quantities in POD theory are measured by the Hilbert-Schmidt norm, see (4).

Lemma 3. *Let $U^j : \mathbb{R}^j \mapsto \mathbb{R}_M^m$ be a given data matrix, $\bar{u}^{j+1} \in \mathbb{R}_M^m$ be a new column data, and U^{j+1} be $[U^j \ \bar{u}^{j+1}] : \mathbb{R}^{j+1} \mapsto \mathbb{R}_M^m$. Then we have $\|U^{j+1}\|_{\text{HS}}^2 = \|U^j\|_{\text{HS}}^2 + \|\bar{u}^{j+1}\|_{\mathbb{R}_M^m}^2$.*

Proof. Simply using Lemma 2, we derive

$$\|U^{j+1}\|_{\text{HS}}^2 = \sum_{i=1}^{j+1} \|\bar{u}^i\|_{\mathbb{R}_M^m}^2 = \sum_{i=1}^j \|\bar{u}^i\|_{\mathbb{R}_M^m}^2 + \|\bar{u}^{j+1}\|_{\mathbb{R}_M^m}^2 = \|U^j\|_{\text{HS}}^2 + \|\bar{u}^{j+1}\|_{\mathbb{R}_M^m}^2.$$

□

As presented in Section 2.2 for the iPOD Algorithm, the data compression errors are from two parts: the p -truncation and SV-truncation. Based on Lemma 3, we estimate these two errors with the following lemmas.

p-truncation error: Let $U^j : \mathbb{R}^j \mapsto \mathbb{R}_M^m$ be a given data matrix and $U^j = V^j \Sigma^j (W^j)^T$ be the core M -weighted SVD. Once a new data \vec{u}^{j+1} is available to be processed, if $p^{j+1} = \|\vec{u}^{j+1} - V^j V^{j*} \vec{u}^{j+1}\|_{\mathbb{R}_M^m}$ is smaller than tol_p , then iPOD will execute a p -truncation, i.e., $\vec{u}^{j+1} \approx V^j V^{j*} \vec{u}^{j+1}$, and update the SVD based on matrix $[U^j \ V^j V^{j*} \vec{u}^{j+1}]$ instead of $[U^j \ \vec{u}^{j+1}]$.

Lemma 4. Let $U^j : \mathbb{R}^j \mapsto \mathbb{R}_M^m$ and $U^j = V^j \Sigma^j (W^j)^T$ be the core M -weighted SVD. Let \vec{u}^{j+1} be a new column data to be processed, $p^{j+1} = \|\vec{u}^{j+1} - V^j V^{j*} \vec{u}^{j+1}\|_{\mathbb{R}_M^m}$, and $\hat{U}^{j+1} = [U^j \ V^j V^{j*} \vec{u}^{j+1}]$. We have

$$\|U^{j+1} - \hat{U}^{j+1}\|_{\text{HS}} = p^{j+1} = \|\vec{u}^{j+1} - V^j V^{j*} \vec{u}^{j+1}\|_{\mathbb{R}_M^m}. \quad (26)$$

Proof. By basic matrix operations and Lemma 3, we have

$$\begin{aligned} \|U^{j+1} - \hat{U}^{j+1}\|_{\text{HS}}^2 &= \|[U^j \ \vec{u}^{j+1}] - [U^j \ V^j V^{j*} \vec{u}^{j+1}]\|_{\text{HS}}^2 \\ &= \|[0 \ \vec{u}^{j+1} - V^j V^{j*} \vec{u}^{j+1}]\|_{\text{HS}}^2 \\ &= \|\vec{u}^{j+1} - V^j V^{j*} \vec{u}^{j+1}\|_{\mathbb{R}_M^m}^2, \end{aligned}$$

which completes the proof. □

SV-truncation error: The second truncation applied to iPOD is the SV-truncation: If the smallest singular value of a data matrix is less than the given threshold tol_{sv} , we truncate it and the corresponding singular vector. The following Lemma estimates this truncation.

Lemma 5. Let $U^j : \mathbb{R}^j \mapsto \mathbb{R}_M^m$, \vec{u}^{j+1} be a new column data to be processed, and \tilde{U}^{j+1} be the approximated data matrix of $U^{j+1} = [U^j \ \vec{u}^{j+1}]$ after applying SV-truncation. If σ_l^{j+1} is the smallest singular value of U^{j+1} that is truncated, then

$$\|U^{j+1} - \tilde{U}^{j+1}\|_{\text{HS}}^2 = (\sigma_l^{j+1})^2.$$

Lemma 5 is a direct implication of Lemma 1.

Based on Lemma 4, Lemma 5, and the lemmas given in Section 2, we provide an incremental way to estimate the error between the exact and compressed data.

Theorem 6. Let \tilde{U}^j and \tilde{U}^{j+1} be the iPOD approximated data matrices of the exact data matrices $U^j : \mathbb{R}^j \mapsto \mathbb{R}_M^m$ and $U^{j+1} = [U^j \ \vec{u}^{j+1}] : \mathbb{R}^{j+1} \mapsto \mathbb{R}_M^m$, respectively. Let $\tilde{U}^j = V^j \Sigma^j (W^j)^T$ be the core M -weighted SVD. If

$$\|U^j - \tilde{U}^j\|_{\text{HS}} \leq \epsilon^j \text{ and } p^{j+1} = \|\vec{u}^{j+1} - V^j V^{j*} \vec{u}^{j+1}\|_{\mathbb{R}_M^m},$$

then

$$\|U^{j+1} - \tilde{U}^{j+1}\|_{\text{HS}} \leq \epsilon^{j+1}, \quad (27)$$

where

$$\epsilon^{j+1} \leq \begin{cases} \epsilon^j & \text{if no truncation is applied,} \\ \epsilon^j + p^{j+1} & \text{if } p\text{-truncation is applied,} \\ \epsilon^j + \sigma_l^{j+1} & \text{if SV-truncation is applied,} \end{cases} \quad (28)$$

and $\{\sigma_i^{j+1}\}_{i=1}^l$ are the singular values of the matrix $[\tilde{U}^j \ \tilde{u}^{j+1}]$.

Proof. Using the triangle inequality and Lemma 4, we deduce

$$\begin{aligned} \|U^{j+1} - \tilde{U}^{j+1}\|_{\text{HS}} &= \|U^{j+1} - [\tilde{U}^j \ \tilde{u}^{j+1}] + [\tilde{U}^j \ \tilde{u}^{j+1}] - \tilde{U}^{j+1}\|_{\text{HS}} \\ &\leq \|U^{j+1} - [\tilde{U}^j \ \tilde{u}^{j+1}]\|_{\text{HS}} + \|[\tilde{U}^j \ \tilde{u}^{j+1}] - \tilde{U}^{j+1}\|_{\text{HS}} \\ &\leq \|U^j - \tilde{U}^j \ 0\|_{\text{HS}} + \|[\tilde{U}^j \ \tilde{u}^{j+1}] - \tilde{U}^{j+1}\|_{\text{HS}} \\ &\leq \|U^j - \tilde{U}^j\|_{\text{HS}} + \|[\tilde{U}^j \ \tilde{u}^{j+1}] - \tilde{U}^{j+1}\|_{\text{HS}}. \end{aligned} \quad (29)$$

According to the inequality (15), each data increment only applies at most one truncation, either p-truncation, SV-truncation, or no truncation. If no truncation is applied, the core M -weighted SVD is updated exactly and the first inequality of (28) holds. If the p-truncation is applied, combining (29) and Lemma 4 gives us

$$\|U^{j+1} - \tilde{U}^{j+1}\|_{\text{HS}} \leq \|U^j - \tilde{U}^j\|_{\text{HS}} + \|\tilde{u}^{j+1} - V^j V^{j*} \tilde{u}^{j+1}\|_{\mathbb{R}_M^m} = \epsilon^j + p^{j+1}. \quad (30)$$

If the SV-truncation is applied, combining (29) and Lemma 5 gives us

$$\|U^{j+1} - \tilde{U}^{j+1}\|_{\text{HS}} \leq \|U^j - \tilde{U}^j\|_{\text{HS}} + \sigma_l^{j+1} \leq \epsilon^j + \sigma_l^{j+1}. \quad (31)$$

This completes the proof. \square

Remark 4. In addition, for one who is interested in the ratio r^{j+1} between the first $j+1$ column approximated data and the exact data, with Lemma 1 and Lemma 2, we can calculate it by

$$r^{j+1} = \sqrt{\frac{\|\tilde{U}^{j+1}\|_{\text{HS}}^2}{\|U^{j+1}\|_{\text{HS}}^2}} = \sqrt{\frac{\|\tilde{U}^{j+1}\|_{\text{HS}}^2}{\sum_{i=1}^{j+1} \|\tilde{u}^i\|_{\mathbb{R}_M^m}^2}} = \sqrt{\frac{\sum_{\{i|\sigma_i^{j+1} \geq \text{tol}_{sv}\}} (\sigma_i^{j+1})^2}{\sum_{i=1}^{j+1} \|\tilde{u}^i\|_{\mathbb{R}_M^m}^2}}. \quad (32)$$

Note that the denominator of the ratio can be computed incrementally so that we do not need to store any data.

Theorem 6 provides us a theoretical approach to set the p -truncation threshold tol_p and the SV-truncation threshold tol_{sv} in the iPOD Algorithm to control the overall data compression error and achieve the desired data approximation accuracy, which additionally implies that the block size of p -truncation data “d” and the number of POD basis vectors in Algorithm 1 are not necessarily pre-defined; they are all automatically determined by the data and the thresholds tol_p and tol_{sv} .

4.2 Gradient error analysis

Recall that the gradient error arises when the compressed data of $\{u_h^n\}_{j=1}^n$ is used to solve the backward adjoint equation (23). To estimate the gradient error, we need to investigate how the data compression error evolves in the backward equation (23). In the following, we analyze such error evolution for example linear and nonlinear PDE constraints, respectively.

We provide a few notations: Let $W^{k,p}(\Omega)$ denote the standard Sobolev spaces, let $H^1(\Omega) = W^{1,2}(\Omega)$ and $L^2(\Omega) = W^{0,2}(\Omega)$, and let $H_0^1(\Omega) = \{v \in H^1(\Omega) : v = 0 \text{ on } \partial\Omega\}$. For presentation convenience, we here consider $V = H_0^1(\Omega)$, $V' = H^{-1}(\Omega)$, $H = L^2(\Omega)$, $\mathcal{H} = L^2(\Omega)$, $\mathcal{U} = L^2(\Omega)$, and the observation operator \mathcal{C} and \mathcal{C}^j to be the identity operator in problem (20)-(21). Then the isomorphism Λ in (23) is an identity operator, and $u_h^{*0}|_{\mathcal{U}_h}$ in (24) is simply u_h^{*0} .

We also recall the Poincaré inequality: $\|v\|_{L^2(\Omega)} \leq C_P \|v\|_{H^1(\Omega)}$ for all $v \in H^1(\Omega)$, where C_P is a positive constant depending on Ω .

4.2.1 Gradient error analysis for a linear PDE constraint

We first consider a linear PDE constraint ($F(u) = 0$ in (21)) to illustrate how the iPOD error impacts the gradient. Again, let $V_h \subset H^1(\Omega)$ denote the finite element space for the considered linear PDE.

Theorem 7. *Assume $F = 0$ and the operator A^* in equation (23) satisfies: $\langle A^*v, v \rangle + C_1 \|v\|_{L^2(\Omega)}^2 \geq C_2 \|v\|_{H^1(\Omega)}^2 \forall v \in H^1(\Omega)$, where $C_1 \geq 0$ and $C_2 > 0$ are constants. Let $\{u_h^j\}$ be solutions of equation (22) with a given initial condition $u_{0,h} \in L^2(\Omega)$ and let $\{\tilde{u}_h^j\}$ be a vector representation of $\{u_h^j\}$. Define the POD operator $U = [\tau^{\frac{1}{2}} \tilde{u}_h^1 \ \tau^{\frac{1}{2}} \tilde{u}_h^2 \ \dots \ \tau^{\frac{1}{2}} \tilde{u}_h^n] : \mathbb{R}^n \mapsto \mathbb{R}_M^m$, where the matrix M is induced by the $L^2(\Omega)$ norm. Let $\tilde{U} = [\tau^{\frac{1}{2}} \tilde{u}_{h,r}^1 \ \tau^{\frac{1}{2}} \tilde{u}_{h,r}^2 \ \dots \ \tau^{\frac{1}{2}} \tilde{u}_{h,r}^n]$ be the approximated data matrix of U by applying the iPOD with respect to the weight matrix M , and ϵ be an error satisfying $\|U - \tilde{U}\|_{\text{HS}} \leq \epsilon$. Denote $C_3 = \frac{2C_1}{1-2C_1\tau}$ and $T = n\tau$. If $1 - 2C_1\tau > 0$, then the gradient error ξ is bounded by*

$$\|\xi\|_{L^2(\Omega)} \leq C_P \sqrt{\frac{e^{C_3 T}}{C_2}} \epsilon. \quad (33)$$

Proof. This is a proof similar to a standard PDE stability analysis with respect to the source term; see Appendix A for details. \square

Remark 5. For parabolic and hyperbolic PDEs, it is typical to have $\langle Av, v \rangle + C_1 \|v\|_{L^2(\Omega)}^2 \geq C_2 \|v\|_{H^1(\Omega)}^2 \quad \forall v \in H^1(\Omega)$, for well-posedness. This property is preserved for A^* because of the linearity of A , i.e., $\langle A^*v, v \rangle + C_1 \|v\|_{L^2(\Omega)}^2 \geq C_2 \|v\|_{H^1(\Omega)}^2 \quad \forall v \in H^1(\Omega)$.

Remark 6. Since the weight matrix M in Theorem 7 is induced by $L^2(\Omega)$ at the discrete level, M is actually the mass matrix in the context of the finite element method. That is, the (i, j) entry of M is actually $\int_{\Omega} \phi_j \phi_i dx dy$, $1 \leq i, j \leq m$, where the $\{\phi_i\}_{i=1}^m$ are the finite element basis functions.

Remark 7. One also can interpret $\sum_{j=1}^n \tau \|v(t_j)\|_0^2$ as a discrete $L^2(\tau, T; L^2(\Omega))$ norm, where $v(t)$ is a piecewise constant function over time $(\tau, T]$. Then minimizing $\sum_{j=1}^n \tau \|u_h^j - u_{h,r}^j\|_0^2$ with an optimal low dimension basis is equivalent to finding the POD of the operator $U = [\bar{u}_h^1 \ \bar{u}_h^2 \ \dots \ \bar{u}_h^n]$ with respect to $L^2(\tau, T; L^2(\Omega))$. This approach leads to a different POD formulation but yields the same data compression, see, e.g., [32].

4.2.2 Gradient error analysis for a nonlinear PDE constraint

The operator $F(\cdot)$ in problem (19) or (20)-(21) is often nonzero as well. Next, we consider the Navier-Stokes equations (NSE) as a typical example of such a nonlinear constraint to analyze the error introduced by iPOD to the gradient. We briefly recall the NSE:

$$\begin{cases} \frac{\partial u}{\partial t} - \nabla \cdot \mathbb{T}(u, p) + (u \cdot \nabla)u = f & \text{in } \Omega \times (0, T], \\ \nabla \cdot u = 0 & \text{in } \Omega \times (0, T], \\ u(\cdot, 0) = u_0 & \text{in } \Omega, \\ u = 0 & \text{on } \partial\Omega, \end{cases} \quad (34)$$

where $u = (u_1 \ u_2)^T$ is velocity in tangential and vertical direction, $\mathbb{T}(u, p) = 2\nu \mathbb{D}(u) - p\mathbb{I}$ is the stress tensor, $\mathbb{D}(u) = \frac{1}{2}(\nabla u + \nabla^T u)$ is the deformation tensor, ν is the kinematic viscosity of the fluid, p is the kinematic pressure, and f is a general external forcing term. At the discrete level, the fully discretized NSE (based on backward Euler and FE spatial discretization) is

$$\begin{cases} \left\langle \frac{u_h^{j+1} - u_h^j}{\tau}, v_h \right\rangle + a(u_h^{j+1}, v_h) + b(u_h^{j+1}, u_h^{j+1}, v_h) + (p_h^{n+1}, \nabla \cdot v_h) \\ = \langle f^{n+1}, v_h \rangle \quad \forall v_h \in V_h, \\ (\nabla \cdot u_h^{j+1}, q_h) = 0 \quad \forall q_h \in Q_h, \\ u_h^0 = u_{0,h} \quad \text{in } L^2(\Omega), \end{cases} \quad (35)$$

for $j = 0, 1, \dots, n-1$. Here, we assume $V_h \times Q_h \subset V \times Q$ is a stable pair of FE spaces that satisfies the inf-sup condition [63, Chapter 4], where $Q = \{q \in L^2(\Omega) : \int_{\Omega} q dx =$

0}. The bilinear form $a(\cdot, \cdot)$ and trilinear form $b(\cdot, \cdot, \cdot)$ are defined as:

$$\begin{aligned} a(u, v) &= (\nu \mathbb{D}(u), \mathbb{D}(v)) = \int_{\Omega} \nu \mathbb{D}(u) \cdot \mathbb{D}(v) dx dy \quad \forall u, v \in V_h, \\ b(u, w, v) &= ((u \cdot \nabla)w, v) = \int_{\Omega} (u \cdot \nabla)w \cdot v dx dy \quad \forall u, w, v \in V_h. \end{aligned}$$

Using the space $V_h^{div} = \{v \in V_h : (q, \nabla \cdot v) = 0 \quad \forall q \in Q_h\}$ and the inf-sup condition, equation (35) is equivalent to

$$\begin{cases} \left\langle \frac{u_h^{j+1} - u_h^j}{\tau}, v_h \right\rangle + a(u_h^{j+1}, v_h) + b(u_h^{j+1}, u_h^{j+1}, v_h) \\ = \langle f^{n+1}, v \rangle \quad \forall v_h \in V_h^{div}, \\ u_h^0 = u_{0,h} \quad \text{in } L^2(\Omega). \end{cases} \quad (36)$$

Then the operators A and $F(\cdot)$ in the problem (20)-(21) are induced by $a(u, v) = \langle Au, v \rangle \quad \forall u, v \in V_h^{div}$ and $b(u, u, v) = \langle F(u), v \rangle \quad \forall u, v \in V_h^{div}$. In addition, the bilinear form $a(\cdot, \cdot)$ has a lower bound by the Korn inequality [64]: Let C_K be a positive constant depending on Ω , then

$$a(v, v) \geq \nu C_K \|\nabla v\|_{L^2(\Omega)} \|\nabla v\|_{L^2(\Omega)} \quad \forall v \in H^1(\Omega). \quad (37)$$

In order to calculate the gradient of the objective function (20) at $u_{0,h}$, we need to first solve the NSE (35) forward and then use the forward solution $\{u_h^j\}$ to solve a backward adjoint equation, for $j = n-1, n-2, \dots, 1, 0$,

$$\begin{cases} \left\langle -\frac{u_h^{*j+1} - u_h^{*j}}{\tau}, v_h \right\rangle + a(u_h^{*j}, v_h) + b(v_h, u_h^{j+1}, u_h^{*j}) \\ + b(u_h^{j+1}, v_h, u_h^{*j}) + (p_h^{*j}, \nabla \cdot v_h) = \langle \hat{u}^{j+1} - u_h^{j+1}, v_h \rangle \quad \forall v_h \in V_h, \\ (\nabla \cdot u_h^{*j}, q_h) = 0 \quad \forall q_h \in Q_h, \\ u_h^{*n} = 0 \quad \text{in } L^2(\Omega). \end{cases} \quad (38)$$

Note that in the above, we have used the fact that the operator A induced by $a(\cdot, \cdot)$ is self-adjoint and $\langle (F'(u_h^{j+1}))^* u_h^{*j}, v_h \rangle = b(v_h, u_h^{j+1}, u_h^{*j}) + b(u_h^{j+1}, v_h, u_h^{*j})$. Then the gradient is given by

$$\nabla J(u_{0,h}) = -u_h^{*0} + \gamma u_{0,h}. \quad (39)$$

Again, the iPOD must be applied for the forward NSE solution data $\{u_h^n\}_{j=1}^n$ to reduce the computer memory requirements. We prove that in this nonlinear problem, the gradient error from iPOD can be bounded if the Hilbert space chosen for the iPOD is $H^1(\Omega)$ instead of $L^2(\Omega)$.

Theorem 8. Let $\{u_h^j\}_{j=1}^n$ be solutions of equation (36) with a given initial condition $u_{0,h} \in L^2(\Omega)$ and $\{\vec{u}_h^j\}_{j=1}^n$ be vector representations of $\{u_h^j\}_{j=1}^n$. Consider the POD operator $U = [\tau^{\frac{1}{2}} \vec{u}_h^1 \ \tau^{\frac{1}{2}} \vec{u}_h^2 \ \dots \ \tau^{\frac{1}{2}} \vec{u}_h^n] : \mathbb{R}^n \mapsto \mathbb{R}_M^m$, where the weight matrix M is induced by $H^1(\Omega)$ norm. Let $\tilde{U} = [\tau^{\frac{1}{2}} \vec{u}_{h,r}^1 \ \tau^{\frac{1}{2}} \vec{u}_{h,r}^2 \ \dots \ \tau^{\frac{1}{2}} \vec{u}_{h,r}^n]$ be the approximated data matrix of U by applying iPOD and let ϵ be an error satisfying $\|U - \tilde{U}\|_{\text{HS}} \leq \epsilon$. If the time step τ is small enough, then the gradient error ξ introduced via iPOD is bounded by

$$\|\xi\|_{L^2(\Omega)} \leq \sqrt{C_4 e^{C_3 T}} \epsilon, \quad (40)$$

where C_3 and C_4 are constants depending on Ω and $\{u_h^{*j}\}_{j=1}^n$ and $\{u_{h,r}^{*j}\}_{j=1}^n$, and $\{u_{h,r}^{*j}\}$ is the solution of (38) replacing $\{u_h^{j+1}\}_{j=0}^{n-1}$ with $\{u_{h,r}^{j+1}\}_{j=0}^{n-1}$.

Remark 8. Theorem 7 and 8 tell us that even under the same objective function, the Hilbert spaces chosen for iPOD data compression may be different due to different PDE constraints.

Remark 9. Since the weight matrix M in Theorem 8 is induced by $H^1(\Omega)$, then for instance, in 2D NSE, $M = \begin{bmatrix} M_1 & 0 \\ 0 & M_1 \end{bmatrix}$, and the (i, j) entry of M_1 is $\int_{\Omega} (\phi_j \phi_i + \nabla \phi_j \nabla \phi_i) dx dy$, $1 \leq i, j \leq m$, where $\{\phi_i\}_{i=1}^m$ are the finite element basis functions.

Proof. Consider the backward equation (38) equipped with the approximated data $\{u_{h,r}^j\}_{j=1}^n$:

$$\begin{cases} \left\langle -\frac{u_{h,r}^{*j+1} - u_{h,r}^{*j}}{\tau}, v_h \right\rangle + a(u_{h,r}^{*j}, v_h) + b(v_h, u_{h,r}^{j+1}, u_h^{*j}) \\ + b(u_{h,r}^{j+1}, v_h, u_h^{*j}) + (p_{h,r}^{*j}, \nabla \cdot v_h) = \langle \hat{u}^{j+1} - u_{h,r}^{j+1}, v_h \rangle, \\ (\nabla \cdot u_{h,r}^{*j}, q_h) = 0, \\ u_h^{*n} = 0, \end{cases} \quad (41)$$

where $u_{h,r}^{*j}$ is the solution at time t_j solved with the approximated data $u_{h,r}^{j+1}$.

Let $e_h^j = u_h^{*j} - u_{h,r}^{*j}$, we subtract (38) from (41) to get the error equation:

$$\begin{cases} \left\langle -\frac{e_h^{j+1} - e_h^j}{\tau}, v_h \right\rangle + a(e_h^j, v_h) + b(v_h, u_h^{j+1}, u_h^{*j}) + b(u_h^{j+1}, v_h, u_h^{*j}) \\ - b(v_h, u_{h,r}^{j+1}, u_{h,r}^{*j}) - b(u_{h,r}^{j+1}, v_h, u_{h,r}^{*j}) + (p_h^{*j} - p_{h,r}^{*j}, \nabla \cdot v_h) \\ = \langle u_{h,r}^{j+1} - u_h^{j+1}, v_h \rangle, \\ (\nabla \cdot e_h^j, q_h) = 0, \\ e_h^n = 0. \end{cases} \quad (42)$$

By adding and subtracting terms, we rewrite the trilinear terms in (42) as

$$\begin{aligned}
& b(v_h, u_h^{j+1}, u_h^{*j}) + b(u_h^{j+1}, v_h, u_h^{*j}) - b(v_h, u_{h,r}^{j+1}, u_{h,r}^{*j}) - b(u_{h,r}^{j+1}, v_h, u_{h,r}^{*j}) \\
&= b(v_h, u_h^{j+1}, u_h^{*j}) - b(v_h, u_{h,r}^{j+1}, u_h^{*j}) + b(v_h, u_{h,r}^{j+1}, u_h^{*j}) \\
&\quad - b(v_h, u_{h,r}^{j+1}, u_{h,r}^{*j}) + b(u_h^{j+1}, v_h, u_h^{*j}) - b(u_h^{j+1}, v_h, u_{h,r}^{*j}) \\
&\quad + b(u_h^{j+1}, v_h, u_{h,r}^{*j}) - b(u_{h,r}^{j+1}, v_h, u_{h,r}^{*j}) \\
&= b(v_h, u_h^{j+1} - u_{h,r}^{j+1}, u_h^{*j}) + b(v_h, u_{h,r}^{j+1}, e_h^j) + b(u_h^{j+1}, v_h, e_h^j) \\
&\quad + b(u_h^{j+1} - u_{h,r}^{j+1}, v_h, u_{h,r}^{*j}).
\end{aligned} \tag{43}$$

Set $v_h = e_h^j$ in (42), since $e_h^j \in V_h^{div}$ and $b(\cdot, e_h^j, e_h^j) = 0$, thus with (43), we have

$$\begin{cases} \left\langle -\frac{e_h^{j+1} - e_h^j}{\tau}, e_h^j \right\rangle + a(e_h^j, e_h^j) + b(e_h^j, u_h^{j+1} - u_{h,r}^{j+1}, u_h^{*j}) \\ + b(e_h^j, u_{h,r}^{j+1}, e_h^j) + b(u_h^{j+1} - u_{h,r}^{j+1}, e_h^j, u_{h,r}^{*j}) = \langle u_{h,r}^{j+1} - u_h^{j+1}, e_h^j \rangle, \\ e_h^n = 0. \end{cases} \tag{44}$$

By using the identity $(a-b)a = \frac{a^2-b^2}{2} + \frac{(a-b)^2}{2}$, Korn's inequality on $a(e_h^j, e_h^j)$, and Cauchy-Schwartz and Young's inequalities on the right side term, we first have

$$\begin{aligned}
& \frac{\|e_h^j\|_{L^2(\Omega)}^2 - \|e_h^{j+1}\|_{L^2(\Omega)}^2}{2} + \frac{\|e_h^j - e_h^{j+1}\|_{L^2(\Omega)}^2}{2} + \tau\nu C_K \|\nabla e_h^j\|_{L^2(\Omega)}^2 \\
& + \tau b(e_h^j, u_h^{j+1} - u_{h,r}^{j+1}, u_h^{*j}) + \tau b(e_h^j, u_{h,r}^{j+1}, e_h^j) + \tau b(u_h^{j+1} - u_{h,r}^{j+1}, e_h^j, u_{h,r}^{*j}) \\
& \leq \frac{\tau}{2} \|u_{h,r}^{j+1} - u_h^{j+1}\|_{L^2(\Omega)}^2 + \frac{\tau}{2} \|e_h^j\|_{L^2(\Omega)}^2.
\end{aligned} \tag{45}$$

The next task is to properly bound the three trilinear terms in (45):

$$\begin{aligned}
& b(e_h^j, u_h^{j+1} - u_{h,r}^{j+1}, u_h^{*j}) \\
& \leq C_1 \|\nabla e_h^j\|_{L^2(\Omega)} \|\nabla(u_h^{j+1} - u_{h,r}^{j+1})\|_{L^2(\Omega)} \|\nabla u_h^{*j}\|_{L^2(\Omega)} \\
& \leq \frac{\nu C_K}{6} \|\nabla e_h^j\|_{L^2(\Omega)}^2 + \frac{3C_1^2}{2\nu C_K} \|\nabla u_h^{*j}\|_{L^2(\Omega)}^2 \|\nabla(u_h^{j+1} - u_{h,r}^{j+1})\|_{L^2(\Omega)}^2, \\
& b(u_h^{j+1} - u_{h,r}^{j+1}, e_h^j, u_{h,r}^{*j}) \\
& \leq C_1 \|\nabla(u_h^{j+1} - u_{h,r}^{j+1})\|_{L^2(\Omega)} \|\nabla e_h^j\|_{L^2(\Omega)} \|\nabla u_{h,r}^{*j}\|_{L^2(\Omega)}
\end{aligned} \tag{46a}$$

$$\leq \frac{\nu C_K}{6} \|\nabla e_h^j\|_{L^2(\Omega)}^2 + \frac{3C_1^2}{2\nu C_K} \|\nabla u_{h,r}^{*j}\|_{L^2(\Omega)}^2 \|\nabla (u_h^{j+1} - u_{h,r}^{j+1})\|_{L^2(\Omega)}^2, \quad (46b)$$

$$\begin{aligned} & b(e_h^j, u_{h,r}^{j+1}, e_h^j) \\ & \leq C_2 \|e_h^j\|_{L^2(\Omega)}^{\frac{1}{2}} \|\nabla e_h^j\|_{L^2(\Omega)}^{\frac{1}{2}} \|\nabla u_{h,r}^{j+1}\|_{L^2(\Omega)} \|\nabla e_h^j\|_{L^2(\Omega)} \\ & = C_2 \|e_h^j\|_{L^2(\Omega)}^{\frac{1}{2}} \|\nabla e_h^j\|_{L^2(\Omega)}^{\frac{3}{2}} \|\nabla u_{h,r}^{j+1}\|_{L^2(\Omega)} \\ & \leq \frac{\nu C_K}{6} \|\nabla e_h^j\|_{L^2(\Omega)}^2 + \left(\frac{9}{2\nu C_K}\right)^3 \frac{C_2^4}{4} \|\nabla u_{h,r}^{j+1}\|_{L^2(\Omega)}^4 \|e_h^j\|_{L^2(\Omega)}^2, \end{aligned} \quad (46c)$$

In the above, we have used the trilinear inequalities [65, Chapter 6] and generalized Young's inequality. Combining (45) and (46) leads to

$$\begin{aligned} & \frac{\|e_h^j\|_{L^2(\Omega)}^2 - \|e_h^{j+1}\|_{L^2(\Omega)}^2}{2} + \frac{\|e_h^j - e_h^{j+1}\|_{L^2(\Omega)}^2}{2} + \tau \frac{\nu C_K}{2} \|\nabla e_h^j\|_{L^2(\Omega)}^2 \\ & \leq \tau \left(\frac{3C_1^2}{2\nu C_K} \|\nabla u_h^{*j}\|_{L^2(\Omega)}^2 + \frac{3C_1^2}{2\nu C_K} \|\nabla u_{h,r}^{*j}\|_{L^2(\Omega)}^2 \right) \|\nabla (u_h^{j+1} - u_{h,r}^{j+1})\|_{L^2(\Omega)}^2 \\ & \quad + \frac{1}{2} \tau \|u_h^{j+1} - u_{h,r}^{j+1}\|_{L^2(\Omega)}^2 + \tau \left(\left(\frac{9}{2\nu C_K}\right)^3 \frac{C_2^4}{4} \|\nabla u_{h,r}^{j+1}\|_{L^2(\Omega)}^4 + \frac{1}{2} \right) \|e_h^j\|_{L^2(\Omega)}^2 \\ & \leq C_4 \tau \|u_h^{j+1} - u_{h,r}^{j+1}\|_{H^1(\Omega)}^2 + \tau \left(\left(\frac{9}{2\nu C_K}\right)^3 \frac{C_2^4}{4} \|\nabla u_{h,r}^{j+1}\|_{L^2(\Omega)}^4 + \frac{1}{2} \right) \|e_h^j\|_{L^2(\Omega)}^2. \end{aligned} \quad (47)$$

Here, $C_4 = \max \left\{ \left(\frac{3C_1^2}{2\nu C_K} \|\nabla u_h^{*j}\|_{L^2(\Omega)}^2 + \frac{3C_1^2}{2\nu C_K} \|\nabla u_{h,r}^{*j}\|_{L^2(\Omega)}^2 \right), \frac{1}{2} \right\}$. Summing (47) over $j = n-1, n-2, \dots, 2, 1, 0$ gives us

$$\begin{aligned} & \|e_h^0\|_{L^2(\Omega)}^2 + \sum_{j=n-1}^0 \left(\|e_h^j - e_h^{j+1}\|_{L^2(\Omega)}^2 + \nu C_K \tau \|\nabla e_h^j\|_0^2 \right) \\ & \leq 2\tau \sum_{j=n-1}^0 \left(\left(\frac{9}{2\nu C_K}\right)^3 \frac{C_2^4}{4} \|\nabla u_{h,r}^{j+1}\|_{L^2(\Omega)}^4 + \frac{1}{2} \right) \|e_h^j\|_{L^2(\Omega)}^2 \\ & \quad + 2C_4 \tau \sum_{j=n-1}^0 \|u_h^{j+1} - u_{h,r}^{j+1}\|_{L^2(\Omega)}^2. \end{aligned} \quad (48)$$

Supposing τ is small enough and using the discrete Gronwall inequality, we have

$$\begin{aligned} & \|e_h^0\|_{L^2(\Omega)}^2 + \sum_{j=n-1}^0 \left(\|e_h^j - e_h^{j+1}\|_{L^2(\Omega)}^2 + \nu C_K \tau \|\nabla e_h^j\|_{L^2(\Omega)}^2 \right) \\ & \leq C_4 e^{C_3 T} \sum_{j=n-1}^0 \tau \|u_h^{j+1} - u_{h,r}^{j+1}\|_{H^1(\Omega)}^2, \end{aligned} \quad (49)$$

$$\text{where } C_3 = \max_{0 \leq j \leq n-1} \left\{ \frac{2 \left(\left(\frac{9}{2\nu C_K} \right)^3 \frac{C_4^4}{4} \|\nabla u_{h,r}^{j+1}\|_{L^2(\Omega)}^4 + \frac{1}{2} \right)}{1 - 2\tau \left(\left(\frac{9}{2\nu C_K} \right)^3 \frac{C_4^4}{4} \|\nabla u_{h,r}^{j+1}\|_{L^2(\Omega)}^4 + \frac{1}{2} \right)} \right\}.$$

Again from (24), the gradient error ξ is actually e_h^0 and is bounded by

$$\|\xi\|_{L^2(\Omega)} = \|e_h^0\|_{L^2(\Omega)} \leq \left(C_4 e^{C_3 T} \sum_{j=n-1}^0 \tau \|u_h^{j+1} - u_{h,r}^{j+1}\|_{H^1(\Omega)}^2 \right)^{\frac{1}{2}}. \quad (50)$$

Based on the POD theory, in order to bound $\left(\sum_{j=n-1}^0 \tau \|u_h^{j+1} - u_{h,r}^{j+1}\|_{H^1(\Omega)}^2 \right)^{\frac{1}{2}}$, we should apply the iPOD for the scaled solution data $\{\tau^{\frac{1}{2}} u_h^j\}_{j=1}^n$ with respect to $H^1(\Omega)$. Consequently, the gradient error has bound

$$\begin{aligned} \|\xi\|_0 &\leq \sqrt{C_4 e^{C_3 T}} \left(\sum_{j=n-1}^0 \|\tau^{\frac{1}{2}} \bar{u}_h^{j+1} - \tau^{\frac{1}{2}} \bar{u}_{h,r}^{j+1}\|_{\mathbb{R}_M^m}^2 \right)^{\frac{1}{2}} \\ &= \sqrt{C_4 e^{C_3 T}} \|U - \tilde{U}\|_{\text{HS}} \leq \sqrt{C_4 e^{C_3 T}} \epsilon, \end{aligned}$$

which completes the proof. \square

Remark 10. *It is worth mentioning that the well-posedness of the forward fully discretized NSE (35) is standard with $u_{0,h} \in L^2(\Omega)$ and $f \in L^\infty(0, T; H^{-1}(\Omega))$. Furthermore, with the FE space $V_h \times Q_h$ (such as P2-P1 Taylor-Hood FE space) and $\tau \leq h$, one can prove that the solution $\{u_h^j\}$ with respect to $H^1(\Omega)$ norm is uniformly bounded by $\|u_{0,h}\|_{L^2(\Omega)}$ and $\|f\|_{L^\infty(0, T; H^{-1}(\Omega))}$ and independent of h and τ [66]. In addition, the wellposedness of both the backward adjoint equations (38) and (41) are not hard to obtain since they are simply linear equations equipped with regular data $\{u_h^j\}$, $\{u_{h,r}^j\}$ and $\{\hat{u}^j\}$. Furthermore, if $\tau \leq h$ the solutions $\{u_h^{*j}\}$ and $\{u_{h,r}^{*j}\}$ can be bounded independent of h and τ and uniformly bounded by $u_{0,h} \in L^2(\Omega)$, $f \in L^\infty(0, T; H^{-1}(\Omega))$, $\{\hat{u}^j\}$, and the iPOD data compression error ϵ . Therefore, the C_3 and C_4 appearing in Theorem 8 are bounded and well-defined constants.*

Remark 11. *In inequalities (A7) and (49), note that $\|e_h^0\|_0$ and the discrete $L^2(0, T; H^1(\Omega))$ error $\tau \sum_{j=n-1}^0 \|e_h^n\|_{H^1(\Omega)}^2$ are bounded by the iPOD data compression error.*

4.3 Convergence analysis for the inexact gradient method

Compared to the usual gradient method, the inexact gradient method contains gradient error in each iteration, which may lead to a lower convergence rate or even divergence. With a given termination tolerance δ , we focus on analyzing the necessary gradient error bound of the inexact gradient method so that it preserves the same convergence rate and also the accuracy of the optimal solution as the usual gradient method; this is the main difference between this work and existing inexact gradient analyses [67–71]. This analysis perspective is especially relevant for time-dependent

PDE-constrained optimization since each iteration needs to solve two PDEs (forward and backward), which is computationally expensive. When lower convergence rates lead to much more iterations, the computation cost is significantly increased. The following analysis will help avoid that. Note that once the gradient error is derived, we can use the analysis results from Sections 4.2.1 and 4.2.2 to accordingly set up the iPOD parameters to achieve such gradient error.

We start with notation. Let X be a Hilbert space and $J : X \mapsto \mathbb{R}$ be a given nonlinear function. Let $J'(x) : X \mapsto \mathbb{R}$ be the linear functional that denotes the first order derivative of $J(x)$ at $x \in X$, $\nabla J(x)$ is the gradient or the dual element of $J'(x)$ in the Hilbert space X so that $\langle J'(x), y \rangle = (\nabla J(x), y)_X$ for all $x, y \in X$.

Recall the inexact gradient method can be generally written as

$$x^{(i+1)} = x^{(i)} - \kappa \left(\nabla J(x^{(i)}) + \xi^{(i)} \right), \quad (51)$$

where, again, κ is the step size of gradient descent and $\xi^{(i)}$ is the gradient error at i^{th} iteration. In our analysis below, we assume the computed gradient is never zero so that $x^{(i+1)} \neq x^{(i)}$.

Definition 3. *Let X be a Hilbert space. A function $J : X \mapsto \mathbb{R}$ is convex if*

$$J(\lambda x + (1 - \lambda)y) \leq \lambda J(x) + (1 - \lambda)J(y) \quad \text{for } \forall x, y \in X \text{ and } \lambda \in [0, 1].$$

Lemma 9. *[67, Appendix B] Let X be a Hilbert space. If the function $J : X \mapsto \mathbb{R}$ is convex and differentiable, then*

$$J(y) \leq J(x) + \langle J'(x), y - x \rangle \quad \forall x, y \in X. \quad (52)$$

Definition 4. *For a Hilbert space X , a function $J : X \mapsto \mathbb{R}$ is L -descent if*

$$J(y) \leq J(x) + \langle J'(x), y - x \rangle + \frac{L}{2} \|y - x\|_X^2 \quad \forall x, y \in X. \quad (53)$$

Remark 12. *Some analysis works on inexact gradient methods assume the function J has a L -Lipschitz continuous gradient. However, the L -descent condition is weaker than this gradient assumption; see [68] for more information.*

Lemma 10. *[72, Chapter 2] Let X be a Hilbert space. If $J : X \mapsto \mathbb{R}$ is differentiable, L -descent, and $\inf J(x) > -\infty$, then*

$$\frac{1}{2L} \|\nabla J(x)\|_X^2 \leq J(x) - \inf J(x) \quad \forall x \in X. \quad (54)$$

Lemma 10 can be proved by setting $y = x - \frac{1}{L} \nabla J(x)$ in (53) and using $\inf J(x) \leq J(x) \quad \forall x \in X$.

Theorem 11. *Let X be a Hilbert space. For the inexact gradient method (51), assume the objective function $J : X \mapsto \mathbb{R}$ is first order differentiable, convex, and L -descent with minimizer $x^* \in X$. Suppose the constant gradient descent step size κ satisfies $0 < \kappa < 1/L$. If for $i = 0, \dots, k-1$ the gradient error in the i th iteration satisfies $\|\xi^{(i)}\|_X <$*

$\frac{2-\kappa L}{4-\kappa L}\|\nabla J(x^{(i)})\|_X$, then the objective function is decreasing, i.e., $J(x^{(i+1)}) < J(x^{(i)})$. In addition, for a given iteration termination tolerance constant δ , choose ϵ so that $\|\xi^{(i)}\|_X \leq \epsilon < \frac{2-\kappa L}{4-\kappa L}\|\nabla J(x^{(i)})\|_X$ for all i and $\delta \geq \|x^{(0)} - x^*\|_X \epsilon + \frac{\kappa \epsilon^2}{2\eta} > 0$, where $\eta = 1 - \kappa L \in (0, 1)$. Then either there exists an i so that the iteration terminates, i.e., $J(x^{(i)}) - J(x^*) < \delta$, or we have

$$J(x^{(k)}) - J(x^*) \leq \frac{1}{2k\kappa}\|x^{(0)} - x^*\|_X^2 + \|x^{(0)} - x^*\|_X \epsilon + \frac{\kappa \epsilon^2}{2\eta}. \quad (55)$$

Proof. First, we derive a gradient error bound to ensure the objective function is decreasing. Taking $y = x^{(i)} - \kappa(\nabla J(x^{(i)}) + \xi^i)$ and $x = x^{(i)}$ in the L-descent inequality (53), we have

$$\begin{aligned} J(x^{(i)} - \kappa(\nabla J(x^{(i)}) + \xi^i)) &\leq J(x^{(i)}) + \left\langle J'(x^{(i)}), -\kappa(\nabla J(x^{(i)}) + \xi^i) \right\rangle \\ &\quad + \frac{L}{2}\|\kappa(\nabla J(x^{(i)}) + \xi^i)\|_X^2 \\ &= J(x^{(i)}) + \left(\nabla J(x^{(i)}) + \xi^i, -\kappa(\nabla J(x^{(i)}) + \xi^i) \right)_X + \frac{L}{2}\|\kappa(\nabla J(x^{(i)}) + \xi^i)\|_X^2 \\ &\quad - \left(\xi^i, -\kappa(\nabla J(x^{(i)}) + \xi^i) \right)_X \\ &= J(x^{(i)}) - (\kappa - \kappa^2 \frac{L}{2})\|\nabla J(x^{(i)}) + \xi^i\|_X^2 - \left(\xi^i, -\kappa(\nabla J(x^{(i)}) + \xi^i) \right)_X \\ &\leq J(x^{(i)}) - \left((\kappa - \kappa^2 \frac{L}{2})\|\nabla J(x^{(i)}) + \xi^i\|_X^2 - \kappa\|\xi^{(i)}\|_X \|\nabla J(x^{(i)}) + \xi^i\|_X \right). \end{aligned} \quad (56)$$

In order to have $J(x^{(i)} - \kappa(\nabla J(x^{(i)}) + \xi^i)) - J(x^{(i)}) < 0$, i.e., $J(x^{(i+1)}) < J(x^{(i)})$, we need based on (56)

$$(\kappa - \kappa^2 \frac{L}{2})\|\nabla J(x^{(i)}) + \xi^i\|_X > \kappa\|\xi^{(i)}\|_X. \quad (57)$$

The inequality (57) can be achieved if the following condition holds

$$(\kappa - \kappa^2 \frac{L}{2})\|\nabla J(x^{(i)}) + \xi^i\|_X \geq (\kappa - \kappa^2 \frac{L}{2})\left(\|\nabla J(x^{(i)})\|_X - \|\xi^i\|_X\right) > \kappa\|\xi^{(i)}\|_X, \quad (58)$$

which leads to

$$\|\xi^{(i)}\|_X < \frac{2-\kappa L}{4-\kappa L}\|\nabla J(x^{(i)})\|_X. \quad (59)$$

Next, we show $\|x^{(i)} - x^*\|_X^2 \leq \|x^{(0)} - x^*\|_X^2$ for all i while $J(x^{(i)}) - J(x^*) \geq \delta$. Based on the inexact gradient iterations, we deduce

$$\|x^{(i+1)} - x^*\|_X^2 - \|x^{(i)} - x^*\|_X^2$$

$$\begin{aligned}
&= -\|x^{(i+1)} - x^{(i)}\|_X^2 - 2\kappa \left(\nabla J(x^{(i)}) + \xi^i, x^{(i+1)} - x^* \right)_X \\
&= -\|x^{(i+1)} - x^{(i)}\|_X^2 - 2\kappa \left(\nabla J(x^{(i)}), x^{(i+1)} - x^{(i)} \right)_X \tag{60}
\end{aligned}$$

$$\begin{aligned}
&+ 2\kappa \left(\nabla J(x^{(i)}), x^* - x^{(i)} \right)_X - 2\kappa \left(\xi^{(i)}, x^{(i+1)} - x^{(i)} \right)_X \\
&- 2\kappa \left(\xi^{(i)}, x^{(i)} - x^* \right)_X. \tag{61}
\end{aligned}$$

Applying the L-descent inequality (53) on $-2\kappa \left(\nabla J(x^{(i)}), x^{(i+1)} - x^{(i)} \right)_X$ gives

$$\begin{aligned}
&- 2\kappa \left(\nabla J(x^{(i)}), x^{(i+1)} - x^{(i)} \right)_X \\
&\leq 2\kappa \left(J(x^{(i)}) - J(x^{(i+1)}) \right) + \kappa L \|x^{(i+1)} - x^{(i)}\|_X^2. \tag{62}
\end{aligned}$$

Using the convexity inequality (52) in Lemma 9 on $2\kappa \left(\nabla J(x^{(i)}), x^* - x^{(i)} \right)_X$ gives

$$2\kappa \left(\nabla J(x^{(i)}), x^* - x^{(i)} \right)_X \leq 2\kappa \left(J(x^*) - J(x^{(i)}) \right). \tag{63}$$

Using Cauchy-Schwartz and Young's inequalities, we obtain upper bounds for the terms $-2\kappa \left(\xi^{(i)}, x^{(i+1)} - x^{(i)} \right)_X$ and $-2\kappa \left(\xi^{(i)}, x^{(i)} - x^* \right)_X$ as follows:

$$\begin{aligned}
-2\kappa \left(\xi^{(i)}, x^{(i+1)} - x^{(i)} \right)_X &\leq 2\kappa \|\xi^{(i)}\|_X \|x^{(i+1)} - x^{(i)}\|_X \\
&\leq \eta \|x^{(i+1)} - x^{(i)}\|_X^2 + \frac{\kappa^2 \|\xi^{(i)}\|_X^2}{\eta}, \tag{64} \\
-2\kappa \left(\xi^{(i)}, x^{(i)} - x^* \right)_X &\leq 2\kappa \|\xi^{(i)}\|_X \|x^{(i)} - x^*\|_X.
\end{aligned}$$

Here, recall $\eta = 1 - \kappa L$ is positive since $\kappa < 1/L$. Combining (60), (62), (63), and (64) leads to

$$\begin{aligned}
&\|x^{(i+1)} - x^*\|_X^2 - \|x^{(i)} - x^*\|_X^2 \\
&\leq -(\eta + \kappa L) \|x^{(i+1)} - x^{(i)}\|_X^2 + \kappa L \|x^{(i+1)} - x^{(i)}\|_X^2 + \eta \|x^{(i+1)} - x^{(i)}\|_X^2 \\
&\quad + \frac{\kappa^2 \|\xi^{(i)}\|_X^2}{\eta} + 2\kappa \|\xi^{(i)}\|_X \|x^{(i)} - x^*\|_X + 2\kappa \left(J(x^*) - J(x^{(i)}) \right) \\
&\quad + 2\kappa \left(J(x^{(i)}) - J(x^{(i+1)}) \right) \tag{65} \\
&\leq 2\kappa \left(\left(J(x^*) - J(x^{(i+1)}) \right) + \|\xi^{(i)}\|_X \|x^{(i)} - x^*\|_X + \frac{\kappa \|\xi^{(i)}\|_X^2}{2\eta} \right).
\end{aligned}$$

Recall $\delta \geq \|x^{(0)} - x^*\|_X \epsilon + \frac{\kappa \epsilon^2}{2\eta}$, and $\|\xi^{(0)}\|_X \leq \epsilon$. Since the iteration is not terminated, we have $J(x^{(1)}) - J(x^*) \geq \delta$ and therefore $(J(x^*) - J(x^{(1)})) + \|\xi^{(0)}\|_X \|x^{(0)} - x^*\|_X \geq \delta$.

$x^* \|_X + \frac{\kappa \|\xi^{(0)}\|_X^2}{2\eta} \leq 0$ and hence $\|x^{(1)} - x^*\|_X^2 \leq \|x^{(0)} - x^*\|_X^2$. By induction, we have that the sequence $\{\|x^{(i)} - x^*\|_X\}_{i \geq 0}$ is non-increasing for all i satisfying $J(x^{(i)}) - J(x^*) \geq \delta$.

Third, we prove the bound (55) in Theorem 11. Define the Lyapunov energy function [73, 74]:

$$E_i = \frac{1}{2\kappa} \|x^{(i)} - x^*\|_X^2 + i \left(J(x^{(i)}) - J(x^*) \right). \quad (66)$$

Since the objective function is decreasing under the condition (59), we hence have with (65)

$$\begin{aligned} E_{i+1} - E_i &= \frac{1}{2\kappa} \|x^{(i+1)} - x^*\|_X^2 + (i+1) \left(J(x^{(i+1)}) - J(x^*) \right) \\ &\quad - \frac{1}{2\kappa} \|x^{(i)} - x^*\|_X^2 - i \left(J(x^{(i)}) - J(x^*) \right) \\ &\leq i \left(J(x^{(i+1)}) - J(x^{(i)}) \right) + \|\xi^{(i)}\|_X \|x^{(i)} - x^*\|_X + \frac{\kappa \|\xi^{(i)}\|_X^2}{2\eta} \\ &\leq \|\xi^{(i)}\|_X \|x^{(i)} - x^*\|_X + \frac{\kappa \|\xi^{(i)}\|_X^2}{2\eta}. \end{aligned}$$

Summing the above inequality from 0 to $k-1$ and using the definition of the energy in (66), we have

$$\begin{aligned} k \left(J(x^{(k)}) - J(x^*) \right) - \frac{1}{2\kappa} \|x^{(0)} - x^*\|_X^2 &\leq E_k - E_0 \\ &= \frac{1}{2\kappa} \|x^{(k)} - x^*\|_X^2 + k \left(J(x^{(k)}) - J(x^*) \right) - \frac{1}{2\kappa} \|x^{(0)} - x^*\|_X^2 \\ &\leq \sum_{i=0}^{k-1} \left(\|\xi^{(i)}\|_X \|x^{(i)} - x^*\|_X + \frac{\kappa \|\xi^{(i)}\|_X^2}{2\eta} \right). \end{aligned} \quad (67)$$

Rearranging (67) and using $\|x^{(i)} - x^*\|_X \leq \|x^{(0)} - x^*\|_X$, we obtain

$$\begin{aligned} J(x^{(k)}) - J(x^*) &\leq \frac{1}{2k\kappa} \|x^{(0)} - x^*\|_X^2 + \sum_{i=0}^{k-1} \frac{\|\xi^{(i)}\|_X \|x^{(i)} - x^*\|_X + \frac{\kappa \|\xi^{(i)}\|_X^2}{2\eta}}{k} \\ &\leq \frac{1}{2k\kappa} \|x^{(0)} - x^*\|_X^2 + \|x^{(0)} - x^*\|_X \epsilon + \frac{\kappa \epsilon^2}{2\eta}. \end{aligned} \quad (68)$$

This completes the proof. \square

Remark 13. Since $\|x^{(i)} - x^*\|_X \leq \|x^{(0)} - x^*\|_X$ is overestimated especially as i increases, then we typically expect

$$\sum_{i=0}^{k-1} \frac{\|\xi^{(i)}\|_X \|x^{(i)} - x^*\|_X + \frac{\kappa \|\xi^{(i)}\|_X^2}{2\eta}}{k} \ll \delta. \quad (69)$$

Actually, better convergence behavior can be proved for the inexact gradient method once stronger smoothness or convexity assumptions are provided on the objective function.

Definition 5. Let X be a Hilbert space, and μ be a positive constant. A function $J : X \mapsto \mathbb{R}$ is said to be μ -**Polyak-Lojasiewicz** if it is bounded below and

$$J(y) - \inf J(x) \leq \frac{1}{2\mu} \|\nabla J(x)\|_X^2 \quad \forall x, y \in X. \quad (70)$$

Definition 6. Let X be a Hilbert space, and μ be a positive constant. A function $J : X \mapsto \mathbb{R}$ is said to be μ -strongly convex if

$$J(y) \geq J(x) + \langle J'(x), y - x \rangle + \frac{\mu}{2} \|y - x\|_X^2 \quad \forall x, y \in X. \quad (71)$$

Theorem 12. Let X be a Hilbert space. For the inexact gradient method (51), assume the objective function $J : X \mapsto \mathbb{R}$ is first order differentiable, μ -**Polyak-Lojasiewicz**, and L -descent with minimizer $x^* \in X$. Denote $\theta = 1 - \mu(2\kappa - L\kappa^2)$. For $\kappa = 1/L$, set ϵ so that the gradient error $\|\xi^{(i)}\|_X \leq \epsilon$ for all $i = 0, 1, 2, \dots, k-1$, then the inexact gradient method (51) satisfies

$$J(x^{(k)}) - J(x^*) \leq \left(1 - \frac{\mu}{L}\right)^k \left(J(x^{(0)}) - J(x^*)\right) + \frac{1}{2\mu} \left(1 - \left(1 - \frac{\mu}{L}\right)^k\right) \epsilon^2. \quad (72)$$

For $0 < \kappa < 1/L$ and $0 < \theta < 1$, set ϵ so that $\|\xi^{(i)}\|_X \leq \epsilon < \frac{2-\kappa L}{4-\kappa L} \|\nabla J(x^{(i)})\|_X$ for all $i = 0, 1, 2, \dots, k-1$, then the inexact gradient method (51) satisfies

$$\begin{aligned} J(x^{(k)}) - J(x^*) &\leq \theta^k \left(J(x^{(0)}) - J(x^*)\right) \\ &+ \frac{1 - \theta^k}{1 - \theta} \left(\sqrt{2L} |L\kappa^2 - \kappa| \sqrt{J(x^{(0)}) - J(x^*)} \epsilon + \frac{L\kappa^2}{2} \epsilon^2\right). \end{aligned} \quad (73)$$

Proof. See Appendix B. □

Theorem 13. Let X be a Hilbert space. For the inexact gradient method (51), assume the objective function $J : X \mapsto \mathbb{R}$ is first order differentiable, μ -strongly convex, and L -descent with minimizer $x^* \in X$. Denote $\theta = 1 - \mu\kappa$ and $\eta = 2\kappa - 2\kappa^2 L$, and suppose the constant gradient descent step size κ satisfies $0 < \kappa < 1/L$. For a given iteration termination tolerance constant δ , set ϵ so that $\|\xi^{(i)}\|_X \leq \epsilon$ for all $i = 0, 1, 2, \dots, k-1$ and $\delta \geq \frac{\sqrt{2L\eta} + \sqrt{2L\eta + 2L\eta\kappa\mu + \kappa\mu}}{\mu\sqrt{2L\eta}} \epsilon > 0$, then the inexact gradient method (51) satisfies

$$\|x^{(k)} - x^*\|_x^2 \leq \theta^k \|x^{(0)} - x^*\|_x^2 + \frac{1 - \theta^k}{1 - \theta} \left(2\kappa \|x^{(0)} - x^*\|_X \epsilon + \frac{\kappa^2}{2L\eta} \epsilon^2 + \kappa^2 \epsilon^2\right). \quad (74)$$

Proof. See Appendix C. □

The first term on the right hand side of inequalities (55), (72), (73), and (74) gives the classical convergence rate of the usual gradient method, while the second term involving ϵ are from the inexact gradient descent iterations. According to a given iteration termination tolerance δ , Theorems 11, 12, and 13 conclude that, if the iPOD parameters are set up properly so that the gradient error ϵ is controlled and the second right-hand side term in the aforementioned inequalities is approximately the same magnitude as δ , the inexact gradient method is expected to achieve the same level accuracy of the optimal solution while using similar number of iterations compared to the usual gradient method. Also, note that the iPOD data compression algorithm only involves small scale matrix and vector multiplications, which is computationally cheap. Hence, the inexact gradient method overall will not largely increase the computation time.

5 Numerical tests

5.1 Linear PDE-constraint optimization test: Data assimilation for a parabolic interface equation

The parabolic interface equations are given by

$$u_t - \nabla \cdot (\beta(x, y) \nabla u) = f \text{ in } \Omega \times (0, T]; \quad u = 0 \text{ on } \partial\Omega \times (0, T]; \quad u(\cdot, 0) = u_0 \text{ in } \Omega, \quad (75)$$

together with jump interface condition $[u]|_\Gamma = g_1$, $[\beta(x, y) \frac{\partial u}{\partial \vec{n}}]|_\Gamma = g_2$. Here, Γ is a smooth curve interface that separates an open bounded domain Ω into two subdomains Ω^+ and Ω^- such that $\Omega = \Omega^+ \cup \Omega^- \cup \Gamma$, $[u]|_\Gamma = u^+|_\Gamma - u^-|_\Gamma$ is the jump of the function u across the interface Γ , $u^+ = u|_{\Omega^+}$ and $u^- = u|_{\Omega^-}$, \vec{n} is the unit normal vector along the interface Γ pointing to Ω^- , $\frac{\partial u}{\partial \vec{n}}$ is the normal derivative of u , and $\beta(x, y)$ is assumed to be a positive piecewise function

$$\beta(x, y) = \begin{cases} \beta^+(x, y) & \text{if } (x, y) \in \Omega^+, \\ \beta^-(x, y) & \text{if } (x, y) \in \Omega^-. \end{cases}$$

In the following experiment, we set the model parameters as $\Omega^+ = (0, 1) \times (0, 1)$, $\Omega^- = (1, 2) \times (0, 1)$, $T = 1$, $\Gamma : x = 1$, $g_1 = g_2 = 0$, $\beta^+ = 1$, $\beta^- = \frac{1}{2}$, and

$$f = \begin{cases} f^+ = ty + x^{\frac{1}{2}} + 5 & \text{in } \Omega^+ \times (0, T], \\ f^- = tx + (xy)^{\frac{1}{2}} + 6 & \text{in } \Omega^- \times (0, T]. \end{cases}$$

In discrete level, we use the backward Euler scheme with $\tau = \frac{1}{500}$ for the temporal discretization and the P2 conforming finite element space V_h with uniform mesh $h = \frac{1}{50}$ for the spatial discretization.

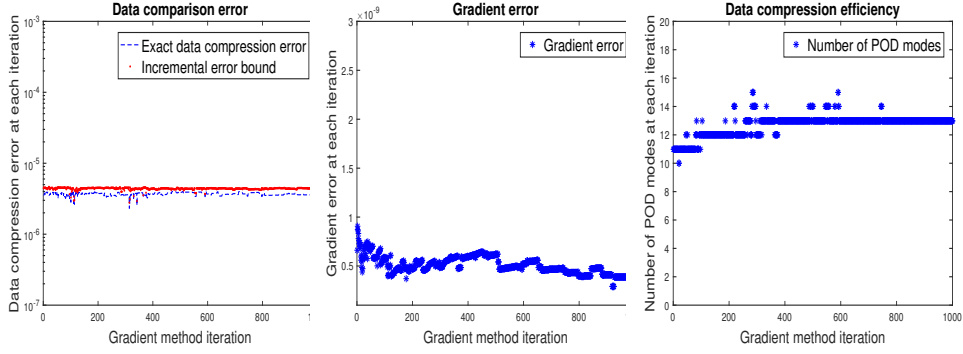


Fig. 1 Linear PDE test 1: Data compression performance

The data assimilation problem is stated as

$$\min_{u_{0,h} \in V_h} J(u_{0,h}) = \frac{1}{2} \tau \sum_{j=1}^n \|\hat{u}^j - u_h^j\|_{L^2(\Omega)}^2 + \frac{\gamma}{2} \|u_{0,h}\|_{L^2(\Omega)}^2, \quad (76)$$

subject to

$$\left\langle \frac{u_h^{j+1} - u_h^j}{\tau}, v_h \right\rangle + a(u_h^{j+1}, v_h) = \langle f^{j+1}, v_h \rangle \quad \forall v_h \in V_h; \quad u_h^0 = u_{0,h} \quad \text{in } L^2(\Omega), \quad (77)$$

for all $j = 0, 1, \dots, n$ and $n = \frac{T}{\tau}$. Here, the bilinear form $a(w, v)$ is defined by $a(w, v) = \int_{\Omega^+} \beta^+ w^+ v dx dy + \int_{\Omega^-} \beta^- w^- v dx dy \quad \forall w, v \in V_h$. According to problem (20)-(21), the operator $F(\cdot)$ here is 0 and the operator A is induced by $\langle Aw, v \rangle = a(w, v) \quad \forall w, v \in V_h$. It is not difficult to verify that $A = A^*$ and $\langle A^*v, v \rangle + C_1 \|v\|_{L^2(\Omega)}^2 \geq C_2 \|v\|_{H^1(\Omega)}^2$.

We choose the observations $\{\hat{u}^j\}$ in (76) as a noisy numerical solution. Specifically, we construct $\{\hat{u}^j\}$ by adding normal noise $e_{ob}^j \sim \mathcal{N}\left(0, \left(\frac{1}{20}I\right)^2\right)$, $j = 1, \dots, N$ onto a numerical solution $\{u_h^j\}$, where the numerical solution is generated by solving the regular parabolic interface equation (77) with the specific initial data $u_{0,h}^+ = \sqrt{xy(2-x)(1-y)}$ in Ω^+ and $u_{0,h}^- = \sqrt{xy(2-x)(1-y)}$ in Ω^- .

We use the gradient Algorithm 2 and inexact gradient Algorithm 3, respectively, to solve for the optimal solution $u_{0,h}^*$ and the corresponding $\{u_h^{j*}\}$ for problem (76)-(77), and test the effectiveness of the inexact gradient method for saving data storage. We set the parameter $\gamma = \frac{1}{2000}$, the step size $\kappa = 1$, and the steepest descent termination criteria $\|\nabla J(u_{0,h}^{(k)})\|_{L(\Omega)} \leq \text{tol}_{sd} = 10^{-5}$. Also, since A is linear and differentiable and the $L^2(\Omega)$ norm is convex and differentiable, the problem (76)-(77) is a linear-quadratic optimization that has enough smoothness and strong convexity. Based on Theorems 6, 7 and 13, to avoid affecting the solution accuracy and the convergence speed from inexact gradient method, we should apply the iPOD with respect to M (that is the mass matrix induced by L^2 norm) and the SVD truncation threshold tol_p and tol_{sv} as 10^{-8} , since we want to have $n\text{tol}_p < 10^{-5}$ and $n\text{tol}_{sv} < 10^{-5}$ so that the data compression error and gradient error are less than $\text{tol}_{sd} = 10^{-5}$.

Table 1 Linear PDE test 1: Comparison between the usual gradient method and the inexact gradient method. $\{u_h^j\}$: exact solution; $\{u_h^{j*}\}$: optimal solution; Relative error:

$$\|u_h - u_h^*\|_{L^2} = \sqrt{\sum_{j=1}^n \tau \|u_h^j - u_h^{j*}\|_{L^2(\Omega)}^2 / \|u_h^j\|_{L^2(\Omega)}^2}.$$

	usual gradient method	inexact gradient method
number of iteration	1001	1001
data storage	10201×500	$\approx 10201 \times 13$
$\ u_h - u_h^*\ _{L^2}$	5.2306×10^{-3}	5.2306×10^{-3}

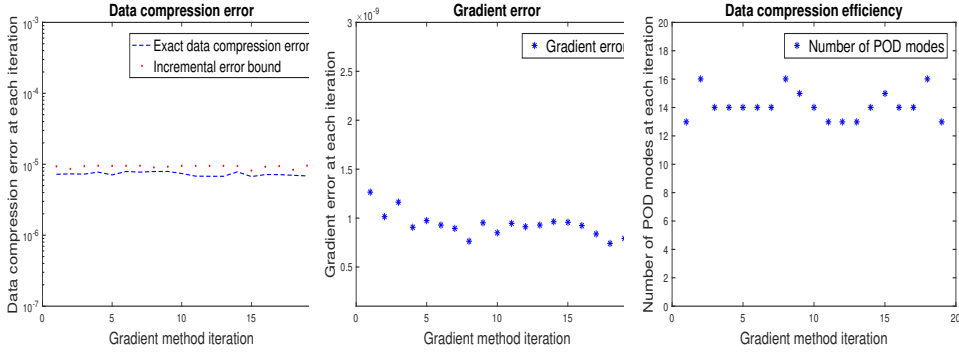


Fig. 2 Linear PDE test 2: Data compression performance

In figure 1, the first plot shows that the error (red dash line) calculated with Theorem 6 is less than 10^{-5} , and the exact data compression error (blue dash line) is sharply bounded by the red line, which verifies that Theorem 6 provides an accurate error estimate for iPOD Algorithm; the second plot shows that the gradient error at each iteration is strictly less than 10^{-5} and thus well-controlled as expected, this verifies Theorem 7; the third plot shows that the inexact gradient method only uses $\frac{13}{500} \times 100 (\approx 2.6)$ percent storage of the usual gradient method. Table 5.1 displays that the inexact gradient method iterates the same number of steps and achieves the same accuracy of the optimal solution compared to the usual gradient method. All these prove the memory efficiency of the inexact gradient method, and also confirms the conclusions in Section 4 (Theorems 7 and 13) that, once the iPOD data compression error and gradient error are properly controlled, the inexact gradient method will have minimal impact on the convergence speed and the solution accuracy.

Moreover, to further test the memory efficiency of the inexact gradient method and the analysis results from Section 4, we run the optimization problem (76)-(77) in a larger scale for a few gradient descent iterations and observe the behaviors. We set $h = \frac{1}{50}$ and $\tau = \frac{1}{2000}$ (with data size: 20402×2000) and $\|\nabla J(u_{0,h}^{(k)})\|_{L(\Omega)} \leq \text{tol}_{sd} = 10^{-5}$. Accordingly, we set $\text{tol}_p = \text{tol}_{sv} = 5 \times 10^{-9}$ to control the data compression error and gradient error. The other parameters are set the same as above. The first two plots in figure 2 show the iPOD data compression error and gradient error are fully controlled as expected by tol_p and tol_{sv} . The third plot in Figure 2 shows that only $\frac{15}{2000} \times 100 (\approx 0.75)$ percent data storage is used compared to usual gradient method. Since the gradient error at each iteration is strictly less than 10^{-5} , we can expect that

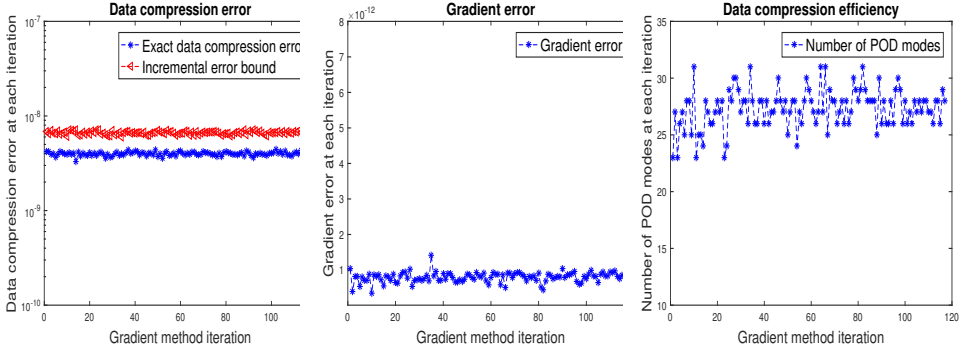


Fig. 3 Nonlinear NSE test 1: Data compression performance

with Theorems 13, the inexact gradient method will not impact the convergence speed and solution accuracy.

5.2 Nonlinear PDE-constraint optimization test: Data assimilation for NSE

We consider a 2D NSE in time-space domain $[0, 1] \times \{[0, 1] \times [-1, 0]\}$ with small viscosity $\nu = \frac{1}{1000}$. We use the backward Euler scheme with $\tau = \frac{1}{500}$ to discretize time and the P2 FE space V_h and the P1 FE space Q_h with uniform mesh $h = \frac{1}{20}$ to discretize the velocity and pressure.

The data assimilation problem is stated as:

$$\min_{u_{0,h} \in V_h} J(u_{0,h}) = \frac{1}{2} \tau \sum_{j=1}^n \|\hat{u}^j - u_h^j\|_{L^2(\Omega)}^2 + \frac{\gamma}{2} \|u_{0,h}\|_{L^2(\Omega)}^2 \quad \text{subject to (35)}. \quad (78)$$

The observations $\{\hat{u}^j\}$ in (78) are given by adding normal noise $e_{ob}^n \sim \mathcal{N}\left(0, \left(\frac{1}{20}I\right)^2\right)$, $j = 1, 2, 3, \dots, N$ onto a numerical solution $\{u_h^j\}$, where the numerical solution is generated by running the regular NSE (35) with initial condition $u_0 = (u_{1,0} \ u_{2,0})^T$. Here, $u_{1,0} = 5xy(1-x)(1+y)$ and $u_{2,0} = 4xy(1-x)(1+y)$.

For the inexact gradient method, based on Theorem 8, we should apply the iPOD with respect to the matrix M that is induced by the H^1 norm to control the gradient error. Although the objective function (78) is smooth, there is not a guarantee that (78) is strongly convex due to the nonlinear constraint. We thus can only assume it is convex and L-descent, which corresponds the case of Theorem 11. If we set the steepest descent termination criteria as $\text{tol}_{sd} = |J(u_{0,h}^{k+1}) - J(u_{0,h}^k)| \leq 10^{-8}$, to avoid hurting the convergence speed and solution accuracy, we need to apply truncation thresholds $\text{tol}_p = \text{tol}_{sv} = 2 \times 10^{-11}$ in iPOD so that the data compression error ($n\text{tol}_p$ and $n\text{tol}_{sv}$) and gradient error do not exceed magnitude 10^{-8} . We also set the parameters $\gamma = \frac{1}{1000}$ and $\kappa = 1$.

In figure 3, the first plot again shows the exact data compression error is sharply bounded by the iPOD error estimate that is calculated with Theorem 6; the second plot

Table 2 Nonlinear NSE test 1: Comparison between the usual gradient method and the inexact gradient method. $\{u_h^j\}$: exact solution; $\{u_h^{j*}\}$: optimal solution; Relative error:

$$\|u_h - u_h^*\|_{\tilde{L}^2} = \sqrt{\sum_{j=1}^n \tau \|u_h^j - u_h^{j*}\|_{L^2(\Omega)}^2 / \|u_h^j\|_{L^2(\Omega)}^2}.$$

	usual gradient method	inexact gradient method
number of iteration	117	117
data storage	3362×500	$\approx 3362 \times 27$
$\ u_h - u_h^*\ _{\tilde{L}^2}$	7.14467×10^{-3}	7.14467×10^{-3}

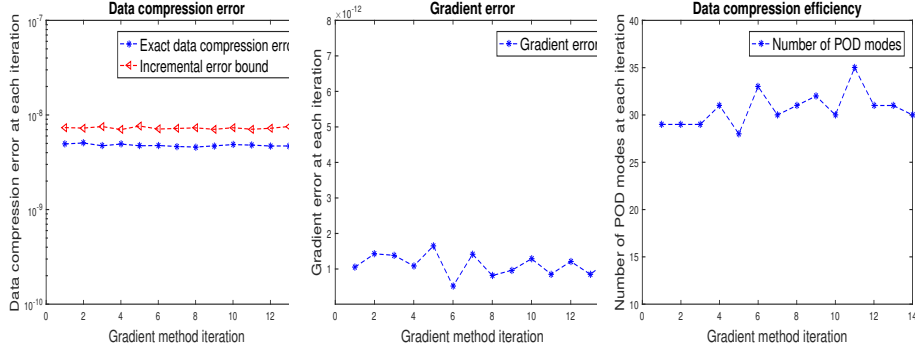


Fig. 4 Nonlinear NSE test 2: Data compression performance

shows that the gradient error is strictly less than 10^{-8} at each iteration as expected, which can always be well bounded by the controllable iPOD data compression error; the third plot shows that the inexact gradient method uses around $\frac{27}{500} \times 100 (\approx 5.4)$ percent storage of the usual gradient method. In addition, Table 5.2 displays that the inexact gradient method achieves the same solution accuracy and convergence speed as the usual gradient method but with much less data storage.

Next, by setting $h = \frac{1}{25}$, $\tau = \frac{1}{1000}$, $\text{tol}_p = \text{tol}_{sv} = 10^{-11}$, $\text{tol}_{sd} = 10^{-8}$, and other parameters the same as above, we run the inexact gradient method for a few iterations in a larger scale with data size 5202×1000 to further test its memory efficiency. Figure 4 shows that the data compression and gradient errors are bounded as desired so that it has minimal impact on solution accuracy and convergence speed. Also, the storage used in the inexact gradient method is around $\frac{32}{1000} \times 100 (\approx 3.2)$ percent of the usual gradient method. All these tests confirm that the inexact gradient method with iPOD is memory efficient and robust.

Remark 14. *It is worth noticing that the gradient errors in tests from Section 5.1 and 5.2 are usually smaller than required, which means in practice we can apply the iPOD truncation thresholds more aggressively to further reduce the data storage required. One simple strategy is to set a truncation threshold and check the corresponding gradient error; if the gradient error is much less than is required, then accordingly increase the iPOD truncation thresholds to further reduce the data storage required. Such a scenario with smaller gradient errors does not contradict the analysis presented here; the analysis holds for even extreme scenarios, but many actual computations are regular cases that yield improved behavior.*

6 Conclusion

We proposed and analyzed an inexact gradient method based on incremental proper orthogonal decomposition to deal with the data storage difficulty in PDE-constrained optimization, and used a data assimilation problem for a detailed illustration. A step-by-step analysis is presented to demonstrate that the inexact gradient method is memory-friendly and robust. In particular, we showed that, with an appropriate iPOD setup, the inexact gradient method is expected to achieve the same level of accuracy of the optimal solution while using a similar number of gradient iterations compared to the usual gradient method. We considered a data assimilation problem for the demonstration of the key ideas. The extension of this work to other types of PDE-constrained optimization problems is interesting future work.

Acknowledgements. Xuejian Li is partially supported by National Science Foundation grants DMS-1722647 and DMS-2111421. John Singler is partially supported by National Science Foundation grant DMS-2111421. Xiaoming He is partially supported by National Science Foundation grants DMS-1722647 and DMS-2152609.

Appendix A Proof of Theorem 7

Proof. To start, we write out the backward equation (23) equipped with the approximated data $\{u_{h,r}^j\}_{j=1}^n$ instead of $\{u_h^j\}_{j=1}^n$:

$$\begin{cases} -\frac{u_{h,r}^{*j+1} - u_{h,r}^{*j}}{\tau} + A^* u_{h,r}^{*j} = \hat{u}^{j+1} - u_{h,r}^{j+1} & \text{in } V_h', \\ u_h^{*n} = 0 & \text{in } L^2(\Omega), \end{cases} \quad (\text{A1})$$

for $j = n-1, \dots, 1, 0$. Here, $u_{h,r}^{*j}$ represents the solution of (A1) at time t_j with approximated data $u_{h,r}^{j+1}$.

Let $e_h^j = u_{h,r}^{*j} - u_h^{*j}$. Subtracting (A1) from (23) and writing the resulting error equation in weak form gives

$$\begin{cases} \left\langle -\frac{e_h^{j+1} - e_h^j}{\tau}, v_h \right\rangle + \langle A^* e_h^j, v_h \rangle = \langle u_h^{j+1} - u_{h,r}^{j+1}, v_h \rangle & \forall v_h \in V_h, \\ e_h^n = 0. \end{cases} \quad (\text{A2})$$

Take $v = e_h^j$ in (A2). Then use the identity $(a-b)a = \frac{a^2-b^2}{2} + \frac{(a-b)^2}{2}$ on the term $\left\langle -\frac{e_h^{j+1} - e_h^j}{\tau}, e_h^j \right\rangle$ and the property $\tau \langle A^* e_h^j, e_h^j \rangle + C_1 \tau \|e_h^j\|_{L^2(\Omega)}^2 \geq \tau C_2 \|e_h^j\|_{H^1(\Omega)}^2$ to obtain

$$\begin{aligned} & \frac{\|e_h^j\|_{L^2(\Omega)}^2 - \|e_h^{j+1}\|_{L^2(\Omega)}^2}{2} + \frac{\|e_h^j - e_h^{j+1}\|_{L^2(\Omega)}^2}{2} + \tau C_2 \|e_h^j\|_{H^1(\Omega)}^2 \\ & \leq \tau C_1 \|e_h^j\|_{L^2(\Omega)}^2 + \tau \langle u_h^{j+1} - u_{h,r}^{j+1}, e_h^j \rangle. \end{aligned} \quad (\text{A3})$$

Applying standard inequalities, such as the Cauchy-Schwartz, Poincaré, and Young's inequalities, yields the following bound for the last term in the right side of (A3):

$$\begin{aligned}
\tau \left\langle u_h^{j+1} - u_{h,r}^{j+1}, e_h^j \right\rangle &\leq \tau \|u_h^{j+1} - u_{h,r}^{j+1}\|_{L^2(\Omega)} \|e_h^j\|_{L^2(\Omega)} \\
&\leq C_P \tau \|u_h^{j+1} - u_{h,r}^{j+1}\|_{L^2(\Omega)} \|e_h^j\|_{H^1(\Omega)} \\
&\leq \frac{C_2}{2} \tau \|e_h^j\|_{H^1(\Omega)}^2 + \frac{C_P^2}{2C_2} \tau \|u_h^{j+1} - u_{h,r}^{j+1}\|_{L^2(\Omega)}^2.
\end{aligned} \tag{A4}$$

Combining (A3) and (A4) leads to

$$\begin{aligned}
&\frac{\|e_h^j\|_{L^2(\Omega)}^2 - \|e_h^{j+1}\|_{L^2(\Omega)}^2}{2} + \frac{\|e_h^j - e_h^{j+1}\|_{L^2(\Omega)}^2}{2} + \frac{C_2}{2} \tau \|e_h^j\|_{H^1(\Omega)}^2 \\
&\leq C_1 \tau \|e_h^j\|_{L^2(\Omega)}^2 + \frac{C_P^2}{2C_2} \tau \|u_h^{j+1} - u_{h,r}^{j+1}\|_{L^2(\Omega)}^2.
\end{aligned} \tag{A5}$$

Summing (A5) over $j = n-1, n-2, \dots, 2, 1, 0$ gives us

$$\begin{aligned}
&\|e_h^0\|_{L^2(\Omega)}^2 + C_2 \tau \sum_{j=n-1}^0 \|e_h^j\|_{H^1(\Omega)}^2 + \sum_{j=n-1}^0 \|e_h^j - e_h^{j+1}\|_{L^2(\Omega)}^2 \\
&\leq 2C_1 \tau \sum_{j=n-1}^0 \|e_h^j\|_{L^2(\Omega)}^2 + \frac{C_P^2}{C_2} \sum_{j=n-1}^0 \tau \|u_h^{j+1} - u_{h,r}^{j+1}\|_{L^2(\Omega)}^2.
\end{aligned} \tag{A6}$$

Denote $C_3 = \frac{2C_1}{1-2C_1\tau}$. Using the assumption $1 - 2C_1\tau > 0$ and the discrete Gronwall inequality on (A6) results in

$$\begin{aligned}
&\|e_h^0\|_{L^2(\Omega)}^2 + C_2 \tau \sum_{j=n-1}^0 \|e_h^j\|_{H^1(\Omega)}^2 + \sum_{j=n-1}^0 \|e_h^j - e_h^{j+1}\|_{L^2(\Omega)}^2 \\
&\leq \frac{e^{C_3 T} C_P^2}{C_2} \sum_{j=n-1}^0 \tau \|u_h^{j+1} - u_{h,r}^{j+1}\|_{L^2(\Omega)}^2.
\end{aligned} \tag{A7}$$

From (24), we note $\nabla J(u_{0,h}) = -u_h^{*0} + \gamma u_{0,h} = -u_{h,r}^{*0} + u_{h,r}^{*0} - u_h^{*0} + \gamma u_{0,h} = -u_{h,r}^{*0} + e_h^0 + \gamma u_{0,h}$, which says that e_h^0 is indeed the gradient error. From POD theory, we know $\left(\sum_{j=n-1}^0 \tau \|u_h^{j+1} - u_{h,r}^{j+1}\|_{L^2(\Omega)}^2\right)^{\frac{1}{2}} = \left(\sum_{j=n-1}^0 \|\tau^{\frac{1}{2}} \bar{u}_h^{j+1} - \tau^{\frac{1}{2}} \bar{u}_{h,r}^{j+1}\|_{\mathbb{R}_M^m}^2\right)^{\frac{1}{2}} = \|U - \tilde{U}\|_{HS}$ with $U : \mathbb{R}^n \mapsto \mathbb{R}_M^m$ and the matrix M is induced by the $L^2(\Omega)$ inner product. Thus, with (A7), we have

$$\|\xi\|_{L^2(\Omega)} = \|e_h^0\|_{L^2(\Omega)} \leq C_P \sqrt{\frac{e^{C_3 T}}{C_2}} \left(\sum_{j=n-1}^0 \|\tau^{\frac{1}{2}} \bar{u}_h^{j+1} - \tau^{\frac{1}{2}} \bar{u}_{h,r}^{j+1}\|_{\mathbb{R}_M^m}^2 \right)^{\frac{1}{2}}$$

$$= C_P \sqrt{\frac{e^{C_3 T}}{C_2}} \|U - \tilde{U}\|_{HS} \leq C_P \sqrt{\frac{e^{C_3 T}}{C_2}} \epsilon,$$

which completes the proof. \square

Appendix B Proof of Theorem 12

Proof. Using the L-descent inequality (53) and the inexact gradient method (51), we deduce

$$\begin{aligned} J(x^{(i+1)}) &\leq J(x^{(i)}) + \left\langle J'(x^{(i)}), x^{(i+1)} - x^{(i)} \right\rangle + \frac{L}{2} \|x^{(i+1)} - x^{(i)}\|_X^2 \\ &= J(x^{(i)}) + \left(\nabla J(x^{(i)}), x^{(i+1)} - x^{(i)} \right)_X + \frac{L}{2} \|x^{(i+1)} - x^{(i)}\|_X^2 \\ &= J(x^{(i)}) + \left(\nabla J(x^{(i)}), -\kappa(\nabla J(x^{(i)}) + \xi^{(i)}) \right)_X + \frac{L\kappa^2}{2} \|\nabla J(x^{(i)}) + \xi^{(i)}\|_X^2 \\ &= J(x^{(i)}) - \kappa \|\nabla J(x^{(i)})\|_X^2 - \kappa \left(\nabla J(x^{(i)}), \xi^{(i)} \right)_X + \frac{L\kappa^2}{2} \|\nabla J(x^{(i)})\|_X^2 \\ &\quad + L\kappa^2 \left(\nabla J(x^{(i)}), \xi^{(i)} \right) + \frac{L\kappa^2}{2} \|\xi^{(i)}\|_X^2 \\ &= J(x^{(i)}) - \left(\kappa - \frac{L\kappa^2}{2} \right) \|\nabla J(x^{(i)})\|_X^2 + (L\kappa^2 - \kappa) \left(\nabla J(x^{(i)}), \xi^{(i)} \right)_X \\ &\quad + \frac{L\kappa^2}{2} \|\xi^{(i)}\|_X^2. \end{aligned} \tag{B8}$$

We discuss the inequality (B8) for two cases based on κ . For $\kappa = \frac{1}{L}$, we have from (B8)

$$J(x^{(i+1)}) \leq J(x^{(i)}) - \frac{1}{2L} \|\nabla J(x^{(i)})\|_X^2 + \frac{1}{2L} \|\xi^{(i)}\|_X^2. \tag{B9}$$

Applying the μ -Polyak-Lojasiewicz inequality (70) and subtracting $J(x^*)$ on both sides of (B9), we obtain

$$J(x^{(i+1)}) - J(x^*) \leq \left(1 - \frac{\mu}{L}\right) \left(J(x^{(i)}) - J(x^*)\right) + \frac{1}{2L} \|\xi^{(i)}\|_X^2. \tag{B10}$$

Unrolling the recursion (B10) gives us

$$J(x^{(k)}) - J(x^*) \leq \left(1 - \frac{\mu}{L}\right)^k \left(J(x^{(0)}) - J(x^*)\right) + \sum_{i=0}^{k-1} \frac{1}{2L} \|\xi^{(i)}\|_X^2 \left(1 - \frac{\mu}{L}\right)^i \tag{B11}$$

$$\leq \left(1 - \frac{\mu}{L}\right)^k \left(J(x^{(0)}) - J(x^*)\right) + \frac{1}{2\mu} \left(1 - \left(1 - \frac{\mu}{L}\right)^k\right) \epsilon^2. \tag{B12}$$

This completes the first part of Theorem 12.

Second, we consider the case: $0 < \kappa < \frac{1}{L}$ and $0 < \mu(2\kappa - L\kappa^2) < 1$. Applying the Cauchy-Schwartz inequality, the μ -**Polyak-Lojasiewicz** inequality (70), and the inequality (54) from Lemma 10 on (B8), we obtain

$$\begin{aligned}
J(x^{(i+1)}) &\leq J(x^{(i)}) - \left(\kappa - \frac{L\kappa^2}{2}\right) \|\nabla J(x^{(i)})\|_X^2 \\
&\quad + |L\kappa^2 - \kappa| \|\nabla J(x^{(i)})\|_X \|\xi^{(i)}\|_X + \frac{L\kappa^2}{2} \|\xi^{(i)}\|_X^2 \\
&\leq J(x^{(i)}) - \mu(2\kappa - L\kappa^2) \left(J(x^{(i)}) - J(x^*)\right) \\
&\quad + \sqrt{2L}|L\kappa^2 - \kappa| \sqrt{J(x^{(i)}) - J(x^*)} \|\xi^{(i)}\|_X + \frac{L\kappa^2}{2} \|\xi^{(i)}\|_X^2.
\end{aligned} \tag{B13}$$

Denote $\theta = 1 - \mu(2\kappa - L\kappa^2)$. Since we assume J is L -descent, $0 < \kappa < 1/L$, and $\|\xi^{(i)}\|_X < \frac{2-\kappa L}{4-\kappa L} \|\nabla J(x^{(i)})\|_X$, Theorem 11 tells us that the function J is decreasing. Then subtracting $J(x^*)$ on both sides of (B13) and using that J is decreasing along iterations gives

$$\begin{aligned}
J(x^{(i+1)}) - J(x^*) &\leq \sqrt{2L}|L\kappa^2 - \kappa| \sqrt{J(x^{(0)}) - J(x^*)} \|\xi^{(i)}\|_X + \frac{L\kappa^2}{2} \|\xi^{(i)}\|_X^2 \\
&\quad + \theta \left(J(x^{(i)}) - J(x^*)\right).
\end{aligned} \tag{B14}$$

Unrolling the recursion (B14) gives us

$$\begin{aligned}
J(x^{(k)}) - J(x^*) &\leq \theta^k \left(J(x^{(0)}) - J(x^*)\right) \\
&\quad + \sum_{i=0}^{k-1} \left(\sqrt{2L}|L\kappa^2 - \kappa| \sqrt{J(x^{(0)}) - J(x^*)} \|\xi^{(i)}\|_X + \frac{L\kappa^2}{2} \|\xi^{(i)}\|_X^2\right) \theta^i \\
&\leq \theta^k \left(J(x^{(0)}) - J(x^*)\right) + \frac{1 - \theta^k}{1 - \theta} \left(\sqrt{2L}|L\kappa^2 - \kappa| \sqrt{J(x^{(0)}) - J(x^*)} \epsilon + \frac{L\kappa^2}{2} \epsilon^2\right),
\end{aligned}$$

which completes the proof. \square

Appendix C Proof of Theorem 13

Proof. Based on the inexact gradient method (51), we have

$$\begin{aligned}
\|x^{(i+1)} - x^*\|_X^2 &= \|x^{(i)} - \kappa \left(\nabla J(x^{(i)}) + \xi^{(i)}\right) - x^*\|_X^2 \\
&= \|x^{(i)} - x^*\|_X^2 - 2\kappa \left(\nabla J(x^{(i)}), x^{(i)} - x^*\right)_X - 2\kappa \left(\xi^{(i)}, x^{(i)} - x^*\right)_X \\
&\quad + \kappa^2 \|\nabla J(x^{(i)})\|_X^2 + 2\kappa \left(\nabla J(x^{(i)}), \xi^{(i)}\right) + \kappa^2 \|\xi^{(i)}\|_X^2.
\end{aligned} \tag{C15}$$

Recall $0 < \kappa < \frac{1}{L}$, then there exists a constant $\eta > 0$ satisfying $2\kappa - 2\kappa^2L - \eta = 0$. Using inequality (71), (54) from Lemma 9, the Cauchy-Schwartz inequality, and Young's inequality we bound (C15) as:

$$\begin{aligned}
& \|x^{(i+1)} - x^*\|_X^2 \leq \|x^{(i)} - x^*\|_X^2 - 2\kappa \left(J(x^{(i)}) - J(x^*) + \frac{\mu}{2} \|x^{(i)} - x^*\|_X^2 \right) \\
& + 2\kappa \|x^{(i)} - x^*\|_X \|\xi^{(i)}\|_X + 2\kappa^2 L \left(J(x^{(i)}) - J(x^*) \right) + \eta \left(J(x^{(i)}) - J(x^*) \right) \\
& + \frac{\kappa^2}{2L\eta} \|\xi^{(i)}\|_X^2 + \kappa^2 \|\xi^{(i)}\|_X^2 \\
& = \|x^{(i)} - x^*\|_X^2 - \left(\kappa\mu \|x^{(i)} - x^*\|_X^2 - 2\kappa \|x^{(i)} - x^*\|_X \|\xi^{(i)}\|_X \right. \\
& \left. - \frac{\kappa^2}{2L\eta} \|\xi^{(i)}\|_X^2 - \kappa^2 \|\xi^{(i)}\|_X^2 \right)
\end{aligned} \tag{C16}$$

Recall $\|\xi^{(i)}\|_X \leq \epsilon$ for all i and $\delta \geq \frac{\sqrt{2L\eta} + \sqrt{2L\eta + 2L\eta\kappa\mu + \kappa\mu}}{\mu\sqrt{2L\eta}} \epsilon$. Since the iteration is not terminated, i.e., $\|x^{(i)} - x^*\|_X \geq \delta$, we then have $-\kappa\mu \|x^{(i)} - x^*\|_X^2 + 2\kappa \|x^{(i)} - x^*\|_X \|\xi^{(i)}\|_X + \frac{8\kappa^2L}{\eta} \|\xi^{(i)}\|_X^2 + \kappa^2 \|\xi^{(i)}\|_X^2 < 0$, and the sequence $\{\|x^{(i)} - x^*\|_X\}_{i \geq 0}$ is non-increasing. Hence, we bound (C16) as

$$\begin{aligned}
& \|x^{(i+1)} - x^*\|_X^2 \leq (1 - \kappa\mu) \|x^{(i)} - x^*\|_X^2 + 2\kappa \|x^{(0)} - x^*\|_X \|\xi^{(i)}\|_X \\
& + \frac{\kappa^2}{2L\eta} \|\xi^{(i)}\|_X^2 + \kappa^2 \|\xi^{(i)}\|_X^2.
\end{aligned} \tag{C17}$$

Denote $\theta = 1 - \mu\kappa$. Unrolling the recursion (C16) gives us

$$\begin{aligned}
& \|x^{(k)} - x^*\|_X^2 \\
& \leq \theta^k \|x^{(0)} - x^*\|_X^2 + \sum_{i=0}^{k-1} \theta^i \left(2\kappa \|x^{(0)} - x^*\|_X \|\xi^{(i)}\|_X + \frac{\kappa^2}{2L\eta} \|\xi^{(i)}\|_X^2 + \kappa^2 \|\xi^{(i)}\|_X^2 \right) \\
& \leq \theta^k \|x^{(0)} - x^*\|_X^2 + \frac{1 - \theta^k}{1 - \theta} \left(2\kappa \|x^{(0)} - x^*\|_X \epsilon + \frac{\kappa^2}{2L\eta} \epsilon^2 + \kappa^2 \epsilon^2 \right),
\end{aligned}$$

which completes the proof. \square

References

- [1] Hinze, M., Kunisch, K.: Second order methods for optimal control of time-dependent fluid flow. SIAM J. Control Optim. **40**(3), 925–946 (2001) <https://doi.org/10.1137/S0363012999361810>
- [2] Gunzburger, M.D., Manservigi, S.: Analysis and approximation of the velocity tracking problem for Navier-Stokes flows with distributed control. SIAM J. Numer. Anal. **37**(5), 1481–1512 (2000) <https://doi.org/10.1137/S0036142997329414>

- [3] Lewis, F.L., Vrabie, D.L., Syrmos, V.L.: Optimal Control. John Wiley & Sons, Hoboken, NJ (2012). <https://doi.org/10.1002/9781118122631> . <https://doi.org/10.1002/9781118122631>
- [4] Lions, J.-L.: Optimal Control of Systems Governed by Partial Differential Equations. Springer, New York-Berlin (1971)
- [5] Athans, M., Falb, P.L.: Optimal Control. An Introduction to the Theory and Its Applications. McGraw-Hill Book Co., New York-Toronto, Ont.-London (1966)
- [6] Altaf, M.U., El Gharamti, M., Heemink, A.W., Hoteit, I.: A reduced adjoint approach to variational data assimilation. *Computer Methods in Applied Mechanics and Engineering* **254**, 1–13 (2013) <https://doi.org/10.1016/j.cma.2012.10.003>
- [7] Gronsksis, A., Heitz, D., Mémin, E.: Inflow and initial conditions for direct numerical simulation based on adjoint data assimilation. *J. Comput. Phys.* **242**, 480–497 (2013) <https://doi.org/10.1016/j.jcp.2013.01.051>
- [8] Daescu, D.N., Navon, I.M.: Efficiency of a POD-based reduced second-order adjoint model in 4D-var data assimilation. *Internat. J. Numer. Methods Fluids* **53**(6), 985–1004 (2007) <https://doi.org/10.1002/fld.1316>
- [9] Ștefănescu, R., Sandu, A., Navon, I.M.: POD/DEIM reduced-order strategies for efficient four dimensional variational data assimilation. *J. Comput. Phys.* **295**, 569–595 (2015) <https://doi.org/10.1016/j.jcp.2015.04.030>
- [10] Yamamoto, M., Zou, J.: Simultaneous reconstruction of the initial temperature and heat radiative coefficient. *Inverse Problems* **17**(4), 1181–1202 (2001) <https://doi.org/10.1088/0266-5611/17/4/340>
- [11] Epanomeritakis, I., Akçelik, V., Ghattas, O., Bielak, J.: A Newton-CG method for large-scale three-dimensional elastic full-waveform seismic inversion. *Inverse Problems* **24**(3), 034015 (2008) <https://doi.org/10.1088/0266-5611/24/3/034015>
- [12] Oberai, A.A., Gokhale, N.H., Feijóo, G.R.: Solution of inverse problems in elasticity imaging using the adjoint method. *Inverse Problems* **19**(2), 297–313 (2003) <https://doi.org/10.1088/0266-5611/19/2/304>
- [13] Bui-Thanh, T., Burstedde, C., Ghattas, O., Martin, J., Stadler, G., Wilcox, L.C.: Extreme-scale UQ for Bayesian inverse problems governed by PDEs. 2012 International Conference for High Performance Computing, Networking, Storage and Analysis (2012) <https://doi.org/10.1109/sc.2012.56>
- [14] Givoli, D.: A tutorial on the adjoint method for inverse problems. *Comput. Methods Appl. Mech. Engrg.* **380**, 113810–23 (2021) <https://doi.org/10.1016/j.cma.2021.113810>

- [15] Hasanov Hasanoglu, A., Romanov, V.G.: Introduction to Inverse Problems for Differential Equations. Springer, Cham (2017). <https://doi.org/10.1007/978-3-319-62797-7>. <https://doi.org/10.1007/978-3-319-62797-7>
- [16] Leeuwen, T., Herrmann, F.J.: A penalty method for PDE-constrained optimization in inverse problems. *Inverse Problems* **32**(1), 015007–26 (2016) <https://doi.org/10.1088/0266-5611/32/1/015007>
- [17] Glowinski, R., Song, Y., Yuan, X., Yue, H.: Bilinear optimal control of an advection-reaction-diffusion system. *SIAM Rev.* **64**(2), 392–421 (2022) <https://doi.org/10.1137/21M1389778>
- [18] Zheng, X., Hu, W., Wu, J.: Numerical algorithms and simulations of boundary dynamic control for optimal mixing in unsteady Stokes flows. *Comput. Methods Appl. Mech. Engrg.* **417**, 116455–24 (2023) <https://doi.org/10.1016/j.cma.2023.116455>
- [19] Wang, Q., Moin, P., Iaccarino, G.: Minimal repetition dynamic checkpointing algorithm for unsteady adjoint calculation. *SIAM J. Sci. Comput.* **31**(4), 2549–2567 (2009) <https://doi.org/10.1137/080727890>
- [20] Charpentier, I.: Checkpointing schemes for adjoint codes: application to the meteorological model Meso-NH. *SIAM J. Sci. Comput.* **22**(6), 2135–2151 (2000) <https://doi.org/10.1137/S1064827598343735>
- [21] Griewank, A.: Achieving logarithmic growth of temporal and spatial complexity in reverse automatic differentiation. *Optimization Methods and Software* **1**(1), 35–54 (1992) <https://doi.org/10.1080/10556789208805505>
- [22] Griewank, A., Walther, A.: Algorithm 799: Revolve. *ACM Transactions on Mathematical Software* **26**(1), 19–45 (2000) <https://doi.org/10.1145/347837.347846>
- [23] Margetis, A.-S.I., Papoutsis-Kiachagias, E.M., Giannakoglou, K.C.: Lossy compression techniques supporting unsteady adjoint on 2D/3D unstructured grids. *Comput. Methods Appl. Mech. Engrg.* **387**, 114152–16 (2021) <https://doi.org/10.1016/j.cma.2021.114152>
- [24] Muthukumar, R., Kouri, D.P., Udell, M.: Randomized sketching algorithms for low-memory dynamic optimization. *SIAM J. Optim.* **31**(2), 1242–1275 (2021) <https://doi.org/10.1137/19M1272561>
- [25] Vezyris, C., Papoutsis-Kiachagias, E., Giannakoglou, K.: On the incremental singular value decomposition method to support unsteady adjoint-based optimization. *Internat. J. Numer. Methods Fluids* **91**(7), 315–331 (2019) <https://doi.org/10.1002/fld.4755>

- [26] Li, X., Hulshoff, S., Hickel, S.: Towards adjoint-based mesh refinement for large eddy simulation using reduced-order primal solutions: preliminary 1D Burgers study. *Comput. Methods Appl. Mech. Engrg.* **379**, 113733–21 (2021) <https://doi.org/10.1016/j.cma.2021.113733>
- [27] Götschel, S., Tycowicz, C., Polthier, K., Weiser, M.: Reducing memory requirements in scientific computing and optimal control. In: *Multiple Shooting and Time Domain Decomposition Methods*. *Contrib. Math. Comput. Sci.*, vol. 9, pp. 263–287. Springer, Cham (2015)
- [28] Heuveline, V., Walther, A.: Online checkpointing for parallel adjoint computation in PDEs: Application to goal-oriented adaptivity and flow control. *Euro-Par 2006 Parallel Processing*, 689–699 (2006) https://doi.org/10.1007/11823285_72
- [29] Brand, M.: Incremental singular value decomposition of uncertain data with missing values. *Computer Vision — ECCV 2002*, 707–720 (2002) <https://doi.org/10.1007/3-540-47969-4-47>
- [30] Fareed, H., Singler, J.R., Zhang, Y., Shen, J.: Incremental proper orthogonal decomposition for PDE simulation data. *Comput. Math. Appl.* **75**(6), 1942–1960 (2018) <https://doi.org/10.1016/j.camwa.2017.09.012>
- [31] Fareed, H., Singler, J.R.: Error analysis of an incremental proper orthogonal decomposition algorithm for PDE simulation data. *J. Comput. Appl. Math.* **368**, 112525–14 (2020) <https://doi.org/10.1016/j.cam.2019.112525>
- [32] Fareed, H., Singler, J.R.: A note on incremental POD algorithms for continuous time data. *Appl. Numer. Math.* **144**, 223–233 (2019) <https://doi.org/10.1016/j.apnum.2019.04.020>
- [33] Kunisch, K., Volkwein, S.: Galerkin proper orthogonal decomposition methods for parabolic problems. *Numer. Math.* **90**(1), 117–148 (2001) <https://doi.org/10.1007/s002110100282>
- [34] Rowley, C.W.: Model reduction for fluids, using balanced proper orthogonal decomposition. *Internat. J. Bifur. Chaos Appl. Sci. Engrg.* **15**(3), 997–1013 (2005) <https://doi.org/10.1142/S0218127405012429>
- [35] Kunisch, K., Volkwein, S.: Galerkin proper orthogonal decomposition methods for a general equation in fluid dynamics. *SIAM J. Numer. Anal.* **40**(2), 492–515 (2002) <https://doi.org/10.1137/S0036142900382612>
- [36] Kunisch, K., Volkwein, S.: Proper orthogonal decomposition for optimality systems. *M2AN Math. Model. Numer. Anal.* **42**(1), 1–23 (2008) <https://doi.org/10.1051/m2an:2007054>
- [37] Rowley, C.W., Colonius, T., Murray, R.M.: Model reduction for compressible

- flows using POD and Galerkin projection. *Phys. D* **189**(1-2), 115–129 (2004) <https://doi.org/10.1016/j.physd.2003.03.001>
- [38] Berkooz, G., Holmes, P., Lumley, J.L.: The proper orthogonal decomposition in the analysis of turbulent flows. In: *Annual Review of Fluid Mechanics*, Vol. 25, pp. 539–575. Annual Reviews, Palo Alto, CA (1993)
- [39] Klus, S., Nüske, F., Koltai, P., Wu, H., Kevrekidis, I., Schütte, C., Noé, F.: Data-driven model reduction and transfer operator approximation. *J. Nonlinear Sci.* **28**(3), 985–1010 (2018) <https://doi.org/10.1007/s00332-017-9437-7>
- [40] Baumann, M., Benner, P., Heiland, J.: Space-time Galerkin POD with application in optimal control of semilinear partial differential equations. *SIAM J. Sci. Comput.* **40**(3), 1611–1641 (2018) <https://doi.org/10.1137/17M1135281>
- [41] Gubisch, M., Volkwein, S.: Proper orthogonal decomposition for linear-quadratic optimal control. In: *Model Reduction and Approximation*. *Comput. Sci. Eng.*, vol. 15, pp. 3–63. SIAM, Philadelphia, PA (2017). <https://doi.org/10.1137/1.9781611974829.ch1> . <https://doi.org/10.1137/1.9781611974829.ch1>
- [42] Gunzburger, M., Jiang, N., Schneier, M.: An ensemble-proper orthogonal decomposition method for the nonstationary Navier-Stokes equations. *SIAM J. Numer. Anal.* **55**(1), 286–304 (2017) <https://doi.org/10.1137/16M1056444>
- [43] Mou, C., Koc, B., San, O., Rebholz, L.G., Iliescu, T.: Data-driven variational multiscale reduced order models. *Comput. Methods Appl. Mech. Engrg.* **373**, 113470–36 (2021) <https://doi.org/10.1016/j.cma.2020.113470>
- [44] Amsallem, D., Zahr, M.J., Farhat, C.: Nonlinear model order reduction based on local reduced-order bases. *Internat. J. Numer. Methods Engrg.* **92**(10), 891–916 (2012) <https://doi.org/10.1002/nme.4371>
- [45] Stange, P.: On the efficient update of the singular value decomposition. *PAMM* **8**(1), 10827–10828 (2008) <https://doi.org/10.1002/pamm.200810827>
- [46] Amsallem, D., Zahr, M.J., Washabaugh, K.: Fast local reduced basis updates for the efficient reduction of nonlinear systems with hyper-reduction. *Adv. Comput. Math.* **41**(5), 1187–1230 (2015) <https://doi.org/10.1007/s10444-015-9409-0>
- [47] Corigliano, A., Dossi, M., Mariani, S.: Model order reduction and domain decomposition strategies for the solution of the dynamic elastic-plastic structural problem. *Comput. Methods Appl. Mech. Engrg.* **290**, 127–155 (2015) <https://doi.org/10.1016/j.cma.2015.02.021>
- [48] Oxberry, G.M., Kostova-Vassilevska, T., Arrighi, W., Chand, K.: Limited-memory adaptive snapshot selection for proper orthogonal decomposition. *Internat. J. Numer. Methods Engrg.* **109**(2), 198–217 (2017) <https://doi.org/10.1002/>

- [49] Schmidt, O.T., Towne, A.: An efficient streaming algorithm for spectral proper orthogonal decomposition. *Comput. Phys. Commun.* **237**, 98–109 (2019) <https://doi.org/10.1016/j.cpc.2018.11.009>
- [50] Zahr, M.J., Farhat, C.: Progressive construction of a parametric reduced-order model for PDE-constrained optimization. *Internat. J. Numer. Methods Engrg.* **102**(5), 1111–1135 (2015) <https://doi.org/10.1002/nme.4770>
- [51] Zimmermann, R., Peherstorfer, B., Willcox, K.: Geometric subspace updates with applications to online adaptive nonlinear model reduction. *SIAM J. Matrix Anal. Appl.* **39**(1), 234–261 (2018) <https://doi.org/10.1137/17M1123286>
- [52] Zhang, Y.: An answer to an open question in the incremental SVD (2022). <https://arxiv.org/abs/2204.05398>
- [53] Singler, J.R.: New POD error expressions, error bounds, and asymptotic results for reduced order models of parabolic PDEs. *SIAM J. Numer. Anal.* **52**(2), 852–876 (2014) <https://doi.org/10.1137/120886947>
- [54] Sirovich, L.: Turbulence and the dynamics of coherent structures. I. Coherent structures. *Quart. Appl. Math.* **45**(3), 561–571 (1987) <https://doi.org/10.1090/qam/910462>
- [55] Gohberg, I., Goldberg, S., Kaashoek, M.A.: Linear operator pencils. *Classes of Linear Operators Vol. I*, 49–58 (1990) https://doi.org/10.1007/978-3-0348-7509-7_5
- [56] Reed, M., Simon, B.: *Methods of Modern Mathematical Physics. I*, 2nd edn. Academic Press, Inc. [Harcourt Brace Jovanovich, Publishers], New York (1980). Functional analysis
- [57] Davies, E.B.: *Linear Operators and Their Spectra*. Cambridge University Press, Cambridge (2007). <https://doi.org/10.1017/CBO9780511618864> . <https://doi.org/10.1017/CBO9780511618864>
- [58] Locke, S., Singler, J.: New proper orthogonal decomposition approximation theory for PDE solution data. *SIAM J. Numer. Anal.* **58**(6), 3251–3285 (2020) <https://doi.org/10.1137/19M1297002>
- [59] Leon, S.J., Bjorck, A., Gander, W.: Gram-schmidt orthogonalization: 100 years and more. *Numerical Linear Algebra with Applications* **20**(3), 492–532 (2012) <https://doi.org/10.1002/nla.1839>
- [60] Manzoni, A., Quarteroni, A., Salsa, S.: *Optimal Control of Partial Differential Equations—analysis, Approximation, and Applications*. Applied Mathematical

- Sciences, vol. 207, p. 498. Springer, Cham ([2021] ©2021). <https://doi.org/10.1007/978-3-030-77226-0> . <https://doi.org/10.1007/978-3-030-77226-0>
- [61] Tröltzsch, F.: Optimal Control of Partial Differential Equations. Graduate Studies in Mathematics, vol. 112, p. 399. American Mathematical Society, Providence, RI (2010). <https://doi.org/10.1090/gsm/112> . Theory, methods and applications, Translated from the 2005 German original by Jürgen Sprekels. <https://doi.org/10.1090/gsm/112>
- [62] Gunzburger, M.D., Hou, L.S.: Finite-dimensional approximation of a class of constrained nonlinear optimal control problems. *SIAM J. Control Optim.* **34**(3), 1001–1043 (1996) <https://doi.org/10.1137/S0363012994262361>
- [63] Girault, V., Raviart, P.-A.: Finite Element Methods for Navier-Stokes Equations. Springer Series in Computational Mathematics, vol. 5, p. 374. Springer, Berlin (1986). <https://doi.org/10.1007/978-3-642-61623-5> . Theory and algorithms. <https://doi.org/10.1007/978-3-642-61623-5>
- [64] Hou, J., Hu, D., Li, X., He, X.: Modeling and a domain decomposition method with finite element discretization for coupled dual-porosity flow and Navier-Stokes flow. *J. Sci. Comput.* **95**(3), 67–45 (2023) <https://doi.org/10.1007/s10915-023-02185-7>
- [65] Layton, W.: Introduction to the Numerical Analysis of Incompressible Viscous Flows. Society for Industrial and Applied Mathematics (SIAM), Philadelphia, PA (2008). <https://doi.org/10.1137/1.9780898718904> . <https://doi.org/10.1137/1.9780898718904>
- [66] Ingimarsen, S., Rebholz, L.G., Iliescu, T.: Full and reduced order model consistency of the nonlinearity discretization in incompressible flows. *Comput. Methods Appl. Mech. Engrg.* **401**, 115620–16 (2022) <https://doi.org/10.1016/j.cma.2022.115620>
- [67] Bertsekas, D.P., Tsitsiklis, J.N.: Gradient convergence in gradient methods with errors. *SIAM J. Optim.* **10**(3), 627–642 (2000) <https://doi.org/10.1137/S1052623497331063>
- [68] Khanh, P.D., Mordukhovich, B.S., Tran, D.B.: Inexact reduced gradient methods in nonconvex optimization. *Journal of Optimization Theory and Applications* (2023) <https://doi.org/10.1007/s10957-023-02319-9>
- [69] Bertsekas, D.P.: Nonlinear Programming, 3rd edn. Athena Scientific Optimization and Computation Series, p. 861. Athena Scientific, Belmont, MA (2016)
- [70] Polyak, B.T., Tsypkin, Y.Z.: Pseudogradient adaptation and training algorithms. *Automat. Remote Control* **34**(3), 377–397 (1973)

- [71] Mangasarian, O.L., Solodov, M.V.: Serial and parallel backpropagation convergence via nonmonotone perturbed minimization. *Optimization Methods and Software* **4**(2), 103–116 (1994) <https://doi.org/10.1080/10556789408805581>
- [72] Garrigos, G., Gower, R.M.: Handbook of convergence theorems for (stochastic) gradient methods (2024). <https://arxiv.org/abs/2301.11235>
- [73] Kalman, R.E., Bertram, J.E.: Control system analysis and design via the “second method” of Lyapunov: I—continuous-time systems. *Journal of Basic Engineering* **82**(2), 371–393 (1960) <https://doi.org/10.1115/1.3662604>
- [74] Wilson, A.C., Recht, B., Jordan, M.I.: A Lyapunov Analysis of Momentum Methods in Optimization. <https://www.arxiv.org/abs/1611.02635>